J 20 419 F

A Publication
for the Radio-Amateur

Especially Covering VHF,
UHF and Microwaves

VHF communications

Volume No. 17 · Winter · 4/1985 · DM 7.00

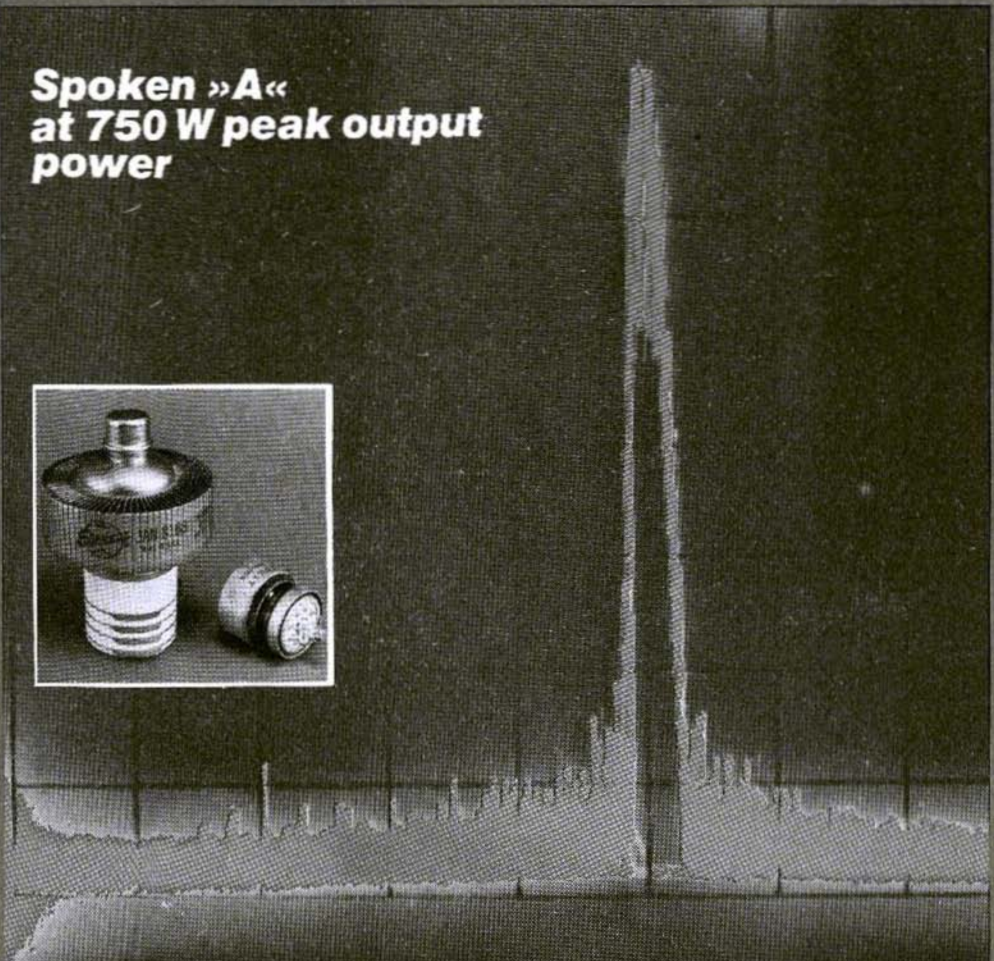

VHF communications

A Publication for the Radio Amateur
Especially Covering VHF, UHF, and Microwaves

Volume No. 17 · Winter · Edition 4/1985

Published by: Verlag UKW-BERICHTE,
Terry Bittan
Jahnstrasse 14
D-8523 BAIERSDORF
Fed. Rep. of Germany
Telephone (9133) 855
Telex 629 887
Postgiro Nbg. 30455-858

Publisher: Verlag UKW-BERICHTE
Terry Bittan

Editors: Corrie Bittan
Colin J. Brock (Assistant)

Translator: Colin J. Brock
G 3 ISB/DJ Ø OK

Advertising manager: Corrie Bittan

VHF COMMUNICATIONS The international edition of the German publication UKW-BERICHTE, is a quarterly amateur radio magazine especially catering for the VHF/UHF/SHF technology. It is published in Spring, Summer, Autumn, and Winter. The 1985 subscription price is DM 24.00 or national equivalent per year. Individual copies are available at DM 7.00 or equivalent, each. Subscriptions, orders of individual copies, purchase of PC-boards and advertised special components, advertisements and contributions to the magazine should be addressed to the national representative, or – if not possible – direct to the publishers.

Printed in the Fed. Rep. of Germany by R. Reichenbach KG. Krelingstr. 39 · 8500 Nuernberg.

We would be grateful if you would address your orders and queries to your representative.

Representatives

Austria
Verlag UKW-BERICHTE, Terry D. Bittan
POB 80, D-8523 Baiersdorf/W.Germany
Creditanstalt Bankverein, WIEN Kto. 17-90.599;
PSchKto WIEN 1.169.146

Australia
W.I.A. P.O.Box 300, South Caulfield, 3162 VIC, Phone 5285962

Belgium
HAM INTERNATIONAL, Brusselsesteenweg 428, B-9218 GENT,
PCR 000-1014257 CCP, Tel.00-32-91-312111

Denmark
Halskov Electronic, OZ7LX, Sigerslevd gamle Skole,
DK-4100 RINGSTED, Telf. 03-616162, Giro 7 29 68 00.

France
Christiane Michel, F 5 SM, SM Electronic,
20 bis, Avenue des Clairions, F-89000 AUXERRE
Tel.(86) 46 96 59

Finland
Erkki Hohenthal, SF-31400 SOMERO
Joensuuntie 6, Tel. 924-46311

Holland
MECOM, PA 0 AER, Postbus 40, Noordwolderweg 12,
NL-9780 AA BEDUM, Tel. 05900-14390.
Postgiro 3986163

Israel
Z. Pomer, 4X4KT, PO Box 222, K. MOZKIN 26114
Tel. 00972-4714078

Italy
Franco Armenghi, I 4 LCK, Via Sigonio 2,
I-40137 BOLOGNA, Tel.(051) 34 56 97

Luxembourg
TELECO, Jos. Faber LX 1 DE, 5–9, Rue de la fontaine
ESCH-SUR-ALZETTE, Tel. 53752

New Zealand
E. M. Zimmermann, ZL 1 AGQ, PO Box 31-261
Milford, AUCKLAND 9, Phone 492-744

Norway
Henning Theg, LA 4 YG, Postboks 70
N-1324 LYSAKER, Postgirokonto 3 16 00 09

South Africa
SA Radio Publications, PO Box 2232, JOHANNES-
BURG 2000, Telephone 011-3378472

Spain + Portugal
Julio A. Prieto Alonso, EA 4 CJ, MADRID-15,
Donoso Cortès 58 5°-B, Tel. 243.83.84

Sweden
Carl-Oscar Biese, SMØHVL, Gjuterribacken 12 B
S-17239 SUNDBYBERG, Tel. 08-29 83 22

Switzerland
Terry Bittan, Schweiz. Kreditanstalt ZÜRICH,
Kto.469.253-41; PSchKto.ZÜRICH 80-54.849

USA
UV COMMS, K3BRS
PO Box 432, LANHAM, MD 20706
Tel. 301-459-4924

ISSN 0177-7505

Contents

UKWberichte Terry D. Bittan · Jahnstr. 14 · Postfach 80 · D-8523 Baiersdorf
Tel. West Germany 9133-855. For Representatives see cover page 2

Friedrich Krug, DJ 3 RV

Micro-Stripline Antennas

In micro stripline circuits discontinuities occur which may be defined as all deviations from the uniform stripline structure such as bends, kinks, branches, impedance transitions, open and short circuits and losses through radiation. Radiation losses increase with frequency, particularly when the geometrical dimensions of the line approach those of an electrical wavelength. This radiation is encouraged in stripline antennas by a suitable arrangement of these discontinuities. Particularly good radiation occurs from power resonators and surface resonators whose electrical dimensions are λ / 2 or multiples thereof. This fact is utilised in other types of antenna.

Micro-stripline antennas are therefore radiating surfaces on a thin dielectric substrate with a conducting ground plane. The main radiation axis is perpendicular to the plane of the radiator.

1. ADVANTAGES AND DISADVANTAGES

Owing to its planer structure the antenna is manufactured by the etching technique in exactly the same manner as for micro-stripline circuits. The demands upon this technique and the materials, particularly for the low-loss dielectric, are very similar. The advantage of these antennas are their uniform, thin structure and negligible weight.

The diagonal measurements of the base plane must, however, be at least a wavelength, and for antenna arrays, considerably larger. The arrangement of many radiation elements into an array results in a greater beam concentration and therefore a higher gain.

Owing to the geometrical dimensional limitations, there has to be a lower frequency restriction of about 300 MHz for these antennas. The upper frequency limit is set by rising conductor losses and losses in the dielectric and is around 30 GHz for PTFE dielectric. Surface wave radiations are also intensified with increasing frequency, particularly when the ratio of substrate thickness to wavelength is greater than 0.1.

Since the radiation surface is driven into resonance, these antennas have a narrower working frequency range than a horn radiator. The obtainable bandwidths range from 1 % to 5 % of the mid-band frequency in the 3 cm band.

The efficiency η is also lower than a horn radiator owing to the higher losses in the thin conductor structure. The gain from a well-matched single element is about 6 dB and with a little more (worthwile) trouble with arrays of elements, gains

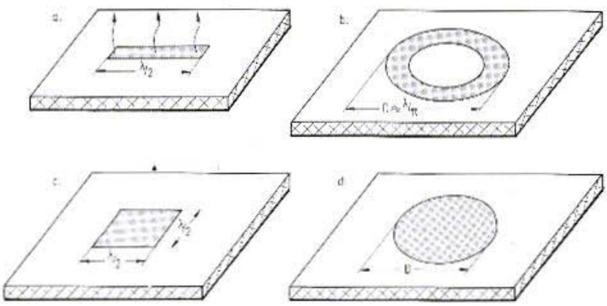

Fig. 1: Surface radiators in micro-stripline technique

of up to 20 dB are possible. The gain, however, is always a few dB lower than the equivalent sized horn antenna would be.

Owing to the negligible power handling capabilities of these antennas, they are not suitable for use as high power radiators. They are almost ideal for receive functions however, as they may be fabricated on the same substrate as say an amplifier with direct low-loss connections – all in the same etching process.

2. FUNCTION

Since the introduction of stripline antennas some 30 years ago a number of technical publications about the subject, and the calculation of fields and radiation conditions, have appeared. For those wishing a more theoretical treatise the reference books (1) and (2) are recommended. They, in turn, provide further references for a deeper study.

In the following article I would like to present a clear description of the micro-stripline antennas together with a few formulae for the approximation of the dimensions.

As already mentioned, conductors radiate particularly powerfully when they complete a $\lambda / 2$ resonate circuit or multiples thereof. Through the nature of the radiating surface and the manner in which they are coupled, they may be categorized into three groups:

The first group encompasses resonant surfaces and conductors and the second are radiating aperatures which to many are known as slot radiators. The third group form travelling wave antennas. The latter comprise a periodic arrangement of discontinuities on a non-radiating feedline which has been properly terminated. As far as the principle function is concerned, travelling wave antennas are similar to surface resonator arrays and will not be considered further.

A few examples of conducting radiating elements are shown in **fig. 1**. A $\lambda / 2$ conductor resonator which produces a linear polarised wave with the E field vector in plane of the antenna is shown in **fig. 1 a**. The ring resonator in **fig. 1 b** represents a closed conductor. The basic oscillitory resonator must have an electrical length of a full wavelength, requiring an average diameter of λ / π. The radiation characteristic and the polarisation, depend upon the way in which it is fed. This applies

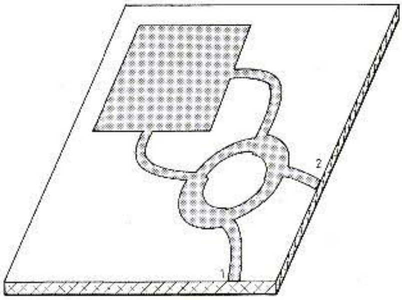

Fig. 2: Circular polarised surface radiator with a 90° hybrid coupler feed in order that the sense of the polarisation may be reversed

also to the surface radiators depicted in 1 c and 1 d as to whether they are linear or circular polarised antennas. The circular polarised radiator must be fed simultaneously on two sides offset physically by 90° by signals having a 90° phase difference between them. The arrangement is shown in **fig. 2**. By the coupling of the surface radiators with a 90° hybrid coupler the polarisation rotational direction may be chosen remotely. If input 1 is fed, and input 2 terminated, the antenna possesses a rigth-handed polarisation and vice-versa a left-handed polarisation is obtained.

The radiating characteristic of the round surface radiator of **fig. 1 d** is dependent upon the type of resonator field which with the aid of cylinder-functions – i. e. approximations to Bessel functions – may be calculated. This cannot be gone into here but references /1/ and /2/ deal with it.

Surface radiator elements may be relatively easily arranged into an array of antennas as **fig. 3** shows. The radiation characteristic and the input impedance of the antenna is determined by the type and phase disposition of the feed. The arrangement in **fig. 3** consists of radiating elements fed in-phase. In the upper diagram $\lambda / 2$ radiating elements are connected by $\lambda / 2$ non-radiating (almost) elements in series so that each radiator leading edge is exactly one wavelength from its neighbour. This means that the antenna is fed in-phase and that the direction of polarisation is in the plane of the antenna.

Fig. 3 lower shows another arrangement of in-phase feeding of radiating elements, the feeder sections are this time, one wavelength long. The polarisation of this arrangement is at right-angles to the feeder section i. e. out of phase by 90° with that of the upper array.

An example of slot radiators is shown in **fig. 4** which depicts two antennas with differing feed arrangements. **Fig. 4 a** shows an arrangement for symmetrical stripline, known as triplate, in which the radiating slot is coupled by a conductor short-circuit. The current is greatest at the short-circuit point and with it the magnetic component of the field which lies at rigth-angles to the plane of the line direction. Since slot antennas have a magnetic field vector which lies in the plane of the antenna, the H field direction of the antenna and that of the short-circuited line are the same so that both slot and line are well coupled.

The arrangement in **4 b** depicts a slot antenna etched in the ground-plane of an unsymmetrical conductor structure and coupled by a micro-stripline which passes over the middle of the slot and at rigth-angles to it. The line is left open-circuited

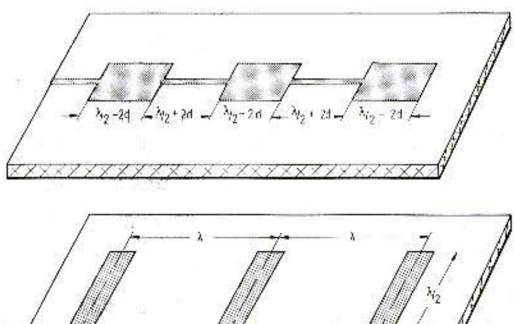

Fig. 3: Antenna arrays consisting of periodically fed radiating elements

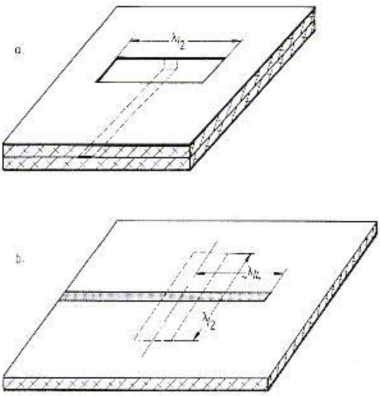

Fig. 4: Examples of slot radiators with H field coupling
a) Triplate configuration with short-circuit coupling
b) Slot radiator in the ground surface with an open-circuit λ / 4 micro-stripline coupling

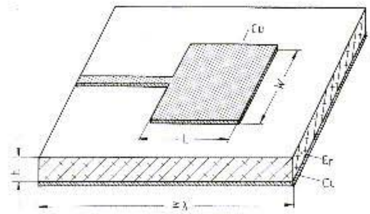

Fig. 5: Rectangular surface radiating elements of length L and width W on a dielectric substrate of thickness h and a complete metal ground screen

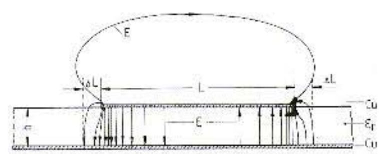

Fig. 6: Cross section through the conductor structure depicting the course and intensity of the electrical field line E

at its end λ / 4 from the middle of the slot. The open-circuit is transformed as a short-circuit in the plane of the slot. The magnetic field component is thereby greatest directly above the slot, which also has its greatest magnetic component at this point, thus providing a good coupling.

The radiation of the slot from the triplate configuration takes place from only one side, the other (ground side) being the reflector. The micro-stripline slot feed arrangement, radiates almost equally in both directions as apposed to the conducting radiators where the metal ground-plane also acts as a radiator, particularly when it has a large area relative to the radiating surface.

3. CALCULATION OF A RECTANGULAR RADIATING ELEMENT

In order to simplify this review, the mathematical details have been omitted but they are available, if required, from ref. /3/.

The surface radiator element shown in **fig. 5** may be regarded as a conductor of length L and width W. Ignore for the moment the narrow feedline and consider it as of length L = λ / 2 i. e. a half-wave resonator.

As the field lines shown in **fig. 6** indicate, at the open-circuit ends, the field is distorted in respect to the ideal field structure along the conductor. This distortion has the effect of elongating the conductor L by the amount $\triangle$ L. This short conductor length is effectively capacitive with a capacitance C. At the same time, the field lines occur in the free-space from end to end of the conductor and the end may be regarded as a radiating slot of length $\triangle$ L and of width W. The radiating energy can be considered to be dissipated through a radiation resistance R so that the surface radiator element may be considered as the equivalent circuit shown in **fig. 7**. It can be seen that the resonant frequency f_0 of the resonator is mainly determined by length L and the effective elongation $\triangle$ L:

(1) $$L = 0{,}5\,\lambda - 2\,\triangle L$$

Since the wave distribution on the conductor is

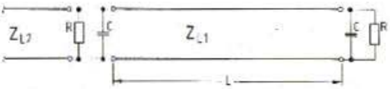

Fig. 7: Equivalent circuit of a radiating element from fig. 5 as a feed-line of characteristic impedance Z_{L1} and the equivalent elements R and C of the open end together with the characteristic impedance Z_{L2}.

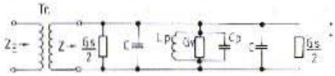

Fig. 8: Equivalent circuit of a micro-stripline radiator in the vicinity of the resonant frequency

Fig. 9: Transformer coupling of a radiating element with a coaxial cable through the ground plane (from /1/)

delayed by the effect of the dielectric, the wavelength is given by

(2) $$\lambda = \lambda_o / \sqrt{\varepsilon_{reff}}$$

where λ_o is the free-space wavelength from

(3) $$\lambda_o = c_o / f_o$$

where c_o = velocity of EM wave in space.

The effective relative permittivity ε_{reff} is dependent upon the conductor width W and the relative permittivity of the substrate. It is given below and in equation /4/ ref. /3/.

(4) $$\varepsilon_{reff} = (\varepsilon_r + 1) / [2 + (\varepsilon_r - 1) \sqrt{4 + 48\,h / W}]$$

The effective elongation $\triangle$ L is calculated as described in ref. /3/ equation /7/.

If the heigth of the substrate $h << \lambda_o$ then $\triangle$ L is approximately: –

(5) $$\triangle L = h / 2$$

The radiation resistance R depends upon the size of the radiating slot and therefore upon the width W of the conductor in relationship to the wavelength.

According to /5/ for the conductor width $W < \lambda / 2$ of the radiation resistance

(6a) $$R = 180\,\Omega / \sqrt{\varepsilon_{reff}} \cdot (\lambda / W)^2$$

and for the conductor width $W > 1.5\,\lambda$ with

(6b) $$R = 240\,\Omega / \sqrt{\varepsilon_{reff}} \cdot (\lambda / W)$$

Since the radiation resistance is effective on both sides of the conductor, the resultant value R_S for one element is:

(7) $$R_s = R / 2$$

The width W of the conductor is calculated as in ref. /3/ which also gives the characteristic impedance Z_{L1} of the resonator element.

For coupling the antenna to the feedline a knowledge of the total impedance Z is necessary and regarding the equivalent circuit of **fig. 8**, the total value of the conductance. This comprises the radiation conductance G_s, a loss conductance G_v, and a susceptance of the equivalent elements of the conductor L_L, C_P and 2 C.

The matching transformer is either accomplished in the feed-line or through coupling into the radiating elements within the length L (**fig. 9**) so that the resonator line itself is used as a transformation element.

For the case of resonance at f_o, the reactive components should fall to zero and the transformed quantities of the radiation conductance and the loss conductance will form the desired input impedance Z_E. In order to have a good antenna efficiency, it is necessary that the loss conductance is very small in relationship to the radiation conductance. Usable micro-stripline antennas are therefore only built with very low-loss dielectrics. The normal micro-stripline materials such as RT/Duroid, Di-Clad or A_2O_3 ceramic, can be considered as practically loss-free up to the 3 cm band. PCB material such as G 10 is unusable above 1 GHz.

Connecting several radiating elements together to form an array, as in **fig. 3**, increases the radiation conductance but also, unfortunately, the loss conductance as well. Additional losses in the connecting lines have the effect of decreasing the ratio of radiation-to-loss conductance. The efficiency of large micro-stripline antenna arrays is so poor that the maximum available gain is limited to 20 dB /6/, /7/ and /8/.

An important criterion of an antenna is its bandwidth, that is, the frequency range in which it is usable. In /1/ the bandwidth for a single radiator was calculated in detail. A knowledge of the material losses is required beforehand, but this can be very tedious for arrays having several radiating elements and coupling networks. A measurement method of determining the bandwidth is very simple and consists of measuring the input impedance versus frequency by means of say, the input VSWR.

The bandwidth Δf will then be defined as the band over which the antenna is suitably matched, i. e. a VSWR of less than say 2 : 1. This can also be expressed as the frequency band over which the return loss is smaller than − 10 dB rel. ref. freq.

Before the measurement is carried out, however, it must be determined that the antenna is beaming in the desired direction in this band of frequencies. It is particularly the case with antenna arrays, it is possible to find that within the usable band and at a frequency at which the VSWR is low, that the radiation beam has slewed off the desired direction or that a side-lobe possesses a greater proportion of the input power. Another possibility, is that the coupling network is matched unintentionally with the loss conductance at this frequency. The radiating elements are then not in resonance and the radiation conductance is negligible. The antenna is then acting as a terminating resistance!

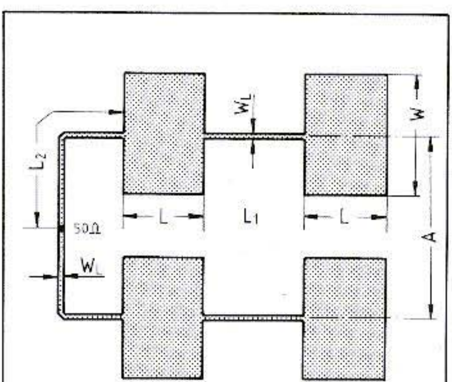

Fig. 10: Antenna array consisting of 2 x 2 rectangular micro-stripline resonators for the 3 cm band

4. CALCULATION AND CONSTRUCTION OF A MICRO-STRIPLINE ANTENNA FOR THE 3 cm BAND

In order to demonstrate the applicability of the formulae, an antenna array consisting of 2 x 2 radiating elements was designed and measured. The array arrangement is shown in **fig. 10**. The array consists of two lines of $\lambda / 2$ radiators, each line having two elements. The polarisation lies in the plane of the feedline L_1.

The radiator length L is determined by the resonant frequency f_o = 10.35 GHz and the width W determines the radiation resistance so that an input impedance of 50 Ω results. In order to have a feed impedance of 50 Ω, each element must have a radiation resistance R_S = 200 Ω on the condition that each element is sufficiently decoupled from the others. The coupling line to the radiator is $L_2 = \lambda$ and has a characteristic impedance of 100 Ω i. e. the impedance of two paralleled radiators.

The construction utilises a teflon substrate RT/ Duroid 5880 with a substrate thickness h = 0.5

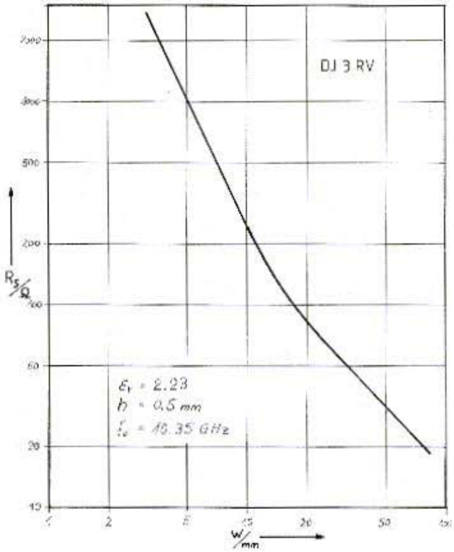

Fig. 11: Radiation resistance R_S of a λ / 2 surface radiator as a function of the conductor width W

mm and 17.5 µm copper film on both sides. The relative permittivity $\varepsilon_r = 2.23$ at 10.35 GHz.

With these material data, a calculation was made for the dimensions L and W of a radiating element as in **fig. 5** at 10.35 GHz and a radiation resistance R_S of 200 Ω. As the radiation resistance lay outside the validity of the formulae **6 a** and **6 b**, the diagram of **fig. 11** was developed. It contains the transitional range of the two formulae as an average value. The diagram directly supplies the radiator width W in millimetres for a given radiation resistance R_S. Now, with the width W, the effective relative permittivity is found with equation (4) and with equation (1) the resonator length L.

The following calculation steps use the diagram from /3/ and the antenna geometrical data for **fig. 10** is listed as follows:

Radiator Width

$R_S = 200\ \Omega \rightarrow$ fig. 11 $\rightarrow \mathbf{W = 11\ mm}$

Radiator Length

$W = 11$ mm $\rightarrow$ with $h = 0.5$ mm $\rightarrow W / h = 22$
$W / h = 22 \rightarrow$ diagram 1 $\rightarrow \varepsilon_{reff} = 2.11$
$f_o = 10.35$ GHz $\rightarrow (2) + (3) \rightarrow \lambda = 19.94$ mm
with $L = 0.5\,\lambda - 2 \triangle L$
$\triangle L$ determined from /3/, diagram /3/
$w / h = 22 \rightarrow$ diagram 3 $\rightarrow d / h = 0.68$
$\triangle L = 0.34$ mm

L = 9.29 mm

The feedlines L_1 and L_2 are loaded with the characteristic impedance $Z_L = 100\ \Omega$.

Line Length L_1

$Z_L \rightarrow$ diagram 2 $\rightarrow W / h = 0.9$
$W / h = 0.9 \rightarrow h = 0.5$ mm $\rightarrow \mathbf{W_L = 0.45\ mm}$
$W / h = 0.9 \rightarrow$ diagram 1 $\rightarrow \varepsilon_{reff} = 1.78$
$f_o = 10.35$ GHz $\rightarrow (2) + (3) \rightarrow \lambda_1 = 21.71$ mm
With $L_1 = 0.5\,\lambda_1 + 2 \triangle L$ for equal phase feeding of both elements.

$\mathbf{L_1 = 11.53\ mm}$

The **distance A** is arbitrary chosen with

$\mathbf{A = L + L_1 = 20.82\ mm}$

For the **Line Length** $_2$, the elongation $\triangle l$ for the compensatory kink as in /3/ as well as the reference plane displacement d_1, must be taken into account. Here the feed point is, (as opposed to fig. 10) a T-branch with 50 Ω feed lines.

$$L_2 = \lambda_1 + \triangle L - 2 \triangle l + d_1$$

This results in the length L_2 along the edge to the middle of the antenna.

$W / h = 0.9 \rightarrow$ /3, eq. (9)/ $\rightarrow 2 \triangle l = 0.013$ mm
$Z_1 = 100\ \Omega$
$Z_2 = 50\ \Omega \rightarrow$ /3, (10) + (11)/ $\rightarrow d_1 = 0.133$ mm

$\mathbf{L_2 = 22.17\ mm}$
b = 0.231 mm from /3/.

5. ANTENNA MEASUREMENTS

The input impedance characteristic with reference to the feed point in **fig. 10** is shown in the

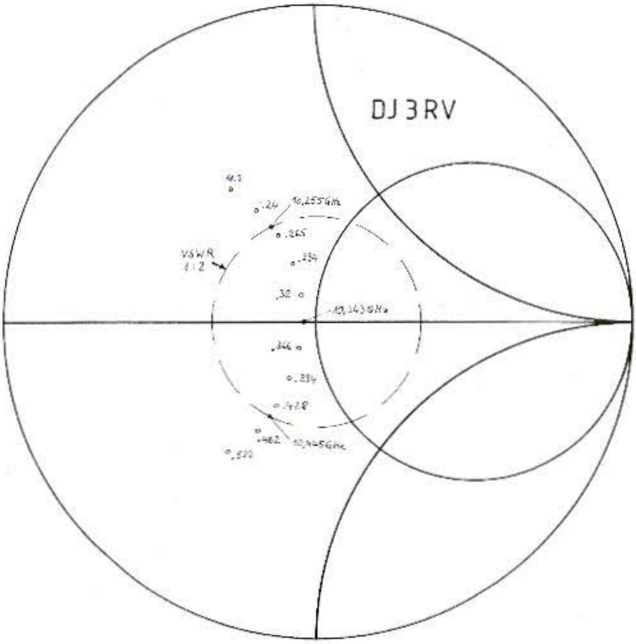

Fig. 12: Feed point input impedance plot on Smith-Chart. The values are for $|r| = 0.1; 0.2; 0.3; 0.4$ and 0.5 at VSWR 1 : 2 ref. 50 Ω

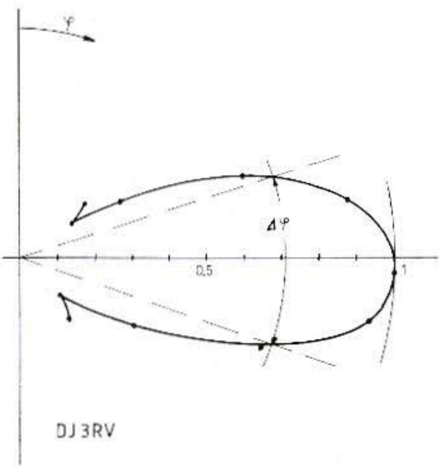

Fig. 13: Directional characteristic in the E-plane (horizontal diagram)

Smith Chart plot in **fig. 12**. The minimal reflection coefficient with

$$r = 0.04\ e^{-180°}$$
$$\text{at } f_o = 10.343 \text{ GHz}$$

This corresponds to an input resistance of

$$Z_E = 46\ \Omega$$

A VSWR = 2 : 1 is measured at 10.255 GHz and 10.445 GHz, giving a bandwidth of 190 MHz i. e. 1,84 %.

Fig. 13 shows the polar plot in the E field plane at f_o = 10.343 GHz. That is the polarisation plane and, normally, the horizontal diagram. It is probably something to do with the feed arrangements that there is a +2° departure from the normal plane symmetry.

The half-power points:

$$\triangle \varphi = +19° \text{ to } -17° = 36°$$

and the first minima occurs at

$$\varphi\, m = +42° \text{ to } -34° = 76°$$

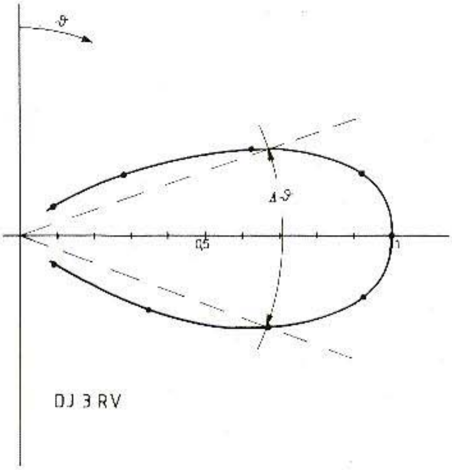

Fig. 14: Directional characteristic in the H-plane (vertical diagram)

Fig. 14 shows the directional characteristic in the H plane at $f_0 = 10.343$ GHz.

The half-power points

$$\triangle \vartheta = +20° \text{ to } -19° = 39°$$

and the first minima occur

$$\vartheta m = +42° \text{ to } -41° = 83°.$$

The **Gain** was measured at $G_i = 10.5$ dB_i

The cross-field polarisation (E component measured in H plane) = − 36 dB (only).

6. REFERENCES

/1/ Bahl, I. J.; Bhartia, P.:
Microstrip Antennas
Artech House, Dedham, Mass. (1980)

/2/ James, J. R.; Hall, P. S.; Wood, C.:
Microstrip Antenna
Theory and Design
IEEE Electromagnetic waves series 12
Peter Pregrinus Ltd., Stevenage (1981)

/3/ Krug, F.:
Formulae and Diagrams for the Approximate Calculation of Micro-Striplines
VHF-COMMUNICATION Vol.17 Ed. 4/1985

/4/ Hammerstad, E. O.:
Equations for Microstrip Circuit Design
Proc. of the 5th EMC, Sept. 1975, P. 268 - 272

/5/ Sobol, H.:
Radiation Conductance of Open-Circuit Microstrip Trans.
MTT - 19. November 1971 P. 885 - 887
and also
Kompa, G.:
Approximate calculation of radiation from open ended wide microstrip lines
Electronics Letters, Vol. 12 1976, P. 22 - 224
Dernesdy, A. G.:
Microstrip Array Antenna Proc. of the 6th EMC, Rom 1976, P. 339 - 343
Wood, C.; Hall, P. S.; James, J. R.:
Radiation conductance of open-circuit low dielectric constant microstrip
Electronic Letters, Vol 14 1978, P. 121 - 123

/6/ Saad, L.:
Eine Streifenleitungs-Richtantenne für den Frequenzbereich 2 bis 40 GHz
Wiss. Berichte AEG-TELEFUNKEN 51 (1978) Heft 2/3, Seite 167 - 176

/7/ Solbach, K.:
Aufbau und Skalierung einer 32-Element Microstrip-Antennen-Gruppe
Mikrowellen-Magazin, 1981,
Heft 4, Seite 461 - 465

/8/ Menzel, W.:
Eine 40-GHz-Mikrostreifenleitungsantenne
Mikrowellen-Magazin, 1981,
Heft 4, Seite 466 - 469

Friedrich Krug, DJ 3 RV

Formulae and Diagrams for the Approximate Calculation of Micro-Striplines

The design and calculation of stripline circuits is still, unfortunately, a specialist's territory. This is partly understandable, as the development of the circuits is more demanding upon the technological possibilities than that for normal printed circuit practice. In spite of this, it is helpful for the understanding of micro-strip circuits, if the impedances of the conductor structure can be determined from its geometry. This will enable anyone with normal radio frequency expertise to, at least, understand the circuit function.

That is the aim of the following presentation of formulae, and in particular, for the understanding and calculation of micro-stripline antennas which are described in this edition of VHF COMMUNICATIONS.

Planar microwave circuits, which are relatively easy to fabricate using etching techniques, mostly employ unsymmetrical striplines. The exact calculation of this type of circuit is very tedious, and in most instances, only possible as an approximation. In order to present a simple method of calculating microwave conducting structures, only the most important approximation formulae from the references /1, /2, /3 have been selected and presented graphically. The diagrams have been calculated based upon the most used substrate, glass-fibre re-inforced PTFE. Types include RT/Duroid 5870 and 5880 Rogers Corp. /4/ or Di-Clad 870 and 880 Keene /5/ with dielectrics constants $\varepsilon_r = 2.32$ and 2.23, resp.

The inaccuracies, consequent upon the approximation approach, are small and well within the tolerances for the dielectric constant and the thickness of the substrate materials. I found that the difference between the calculated results and the actual measured results lay within $\pm$ 3 %. This is not normally critical for simple circuits (filters and resonators), however, a correction may have to be applied. The fabrication must also be carefully controlled, as the design of the mask, application of the photo sensitive resist, the exposure, development and etching all influence the width of the conductor tracks. These manufacturing tolerances must be known and taken into account.

1. CONDUCTOR WIDTH

Fig. 1 shows a cross-sectional view of a micro-strip conductor of width W and conductor thickness t, etched from a board of dielectric thickness h and relative dielectric constant ε_r. The conducting ground plane is continuous. The calculation

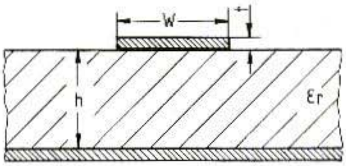

Fig. 1: Cross-section through a micro-stripline

of the conductor dimensions is accomplished by the aid of /3/ **equation (1)** using the application range $\varepsilon_r \leq 16$ and $0.5 \leq W / h \leq 20$ assuming $t = 0$ and neglecting frequency. They supply for the desired conductor characteristic impedance Z_L the ratio of track width to substrate thickness W / h

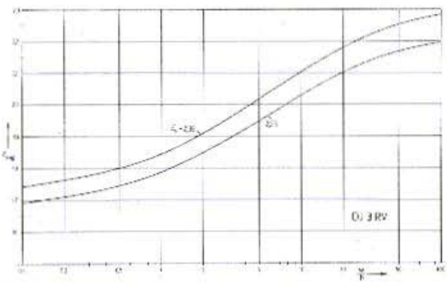

Diagram 1: Effective relative permittivity ε_{reff} as a function of W/h for an ε_r of 2.23 and 2.32

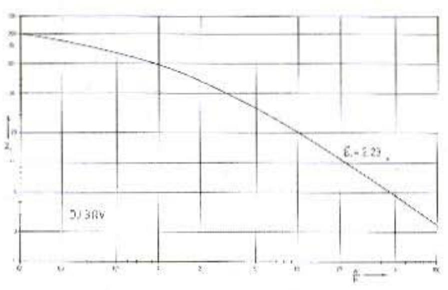

Diagram 2: Characteristic impedance Z_L of a stripline as a function of W/h for $\varepsilon_r = 2.23$. The displacement of Z_L for $\varepsilon_r = 2.32$ is small enough to be neglected and cannot therefore be shown as a seperate curve.

for the given dielectric constant ε_r of the substrate material. **Equation (2)** supplies the effective dielectric constant ε_{reff} i. e. the modified value due to lines of force fringing.

For an overall view, the values for $\varepsilon_r = 2.23$ and $\varepsilon_r = 2.32$ are depicted in **diagram 1** as a function of W / h.

The conductor characteristic impedance Z_L may be calculated with the aid of **equation (3)** from the given geometrical dimensions. These values for the impedance Z_L are plotted against the ratio W / h for $\varepsilon_r = 2.23$ in **diagram 2**. The values for the characteristic impedance Z_L at $\varepsilon_r = 2.32$ lie about 2 % lower and cannot be clearly depicted in the diagram.

The influence of the conductor track thickness t has been neglected in **equation (1) to (3)** but the error is very small for track thicknesses from 17.5 μm to 35 μm. Thick conductor tracks also very narrow tracks, exhibit greater lines-of-force fringing effects and the effective dielectric constant is therefore smaller. This factor can be taken into account with **equation (4) and (5)** from /1/. The resulting corrected value for ε_{reff}^* and conductor width W* are used in **equation (3)** to obtain an improved value for the characteristic impedance. The conditions $h >> t$; $2\,t < W$ and $t < 0.75\,(W^* - W)$ must, however, be observed.

The influence of frequency is dertermined by /2/ **equation (6)**. This supplies a frequency corrected effective dielectric permittivity $\varepsilon_{reff}(f)$ which at 10 GHz and with PTFE substrate is about 2 % higher than determined by **equation (2)**.

2. END CAPACITANCE OF AN OPEN-CIRCUIT LINE

An open-circuited micro-stripline has, at its end, a fringe field which has a capacitive effect. This tends to give the conductor a greater electrical length than its physical length by an amount d.

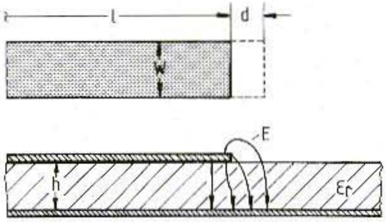

Fig. 2: Additional length d of an open-circuit stripline caused by the fringing of the E field at its end

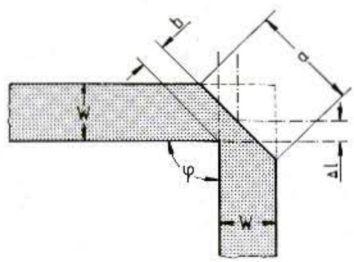

Fig. 3: Compensation of the fringing effect at a bend by cutting off the corner

Fig. 2 shows this fringing field and the resultant elongation d. This effect must be taken into account e. g. with probes or resonators in **equation (7)** from /2/ and is valid for $0.01 \leq W/h \leq 100$ and $1 \leq \varepsilon_r < 50$. The curve is shown in **diagram 3** for $\varepsilon_r = 2.23$.

3. COMPENSATING DEVICES

When designing microstrip circuits, it is frequently necessary to form an angle φ in the track to change direction. A bend is formed as shown in **fig. 3**, which also possesses a fringing field which adds an effective additional capacity. A relatively wide-band compensation method is to cut the corner as in **fig. 3**. In /1/ a corner-cut of length a = 1.8

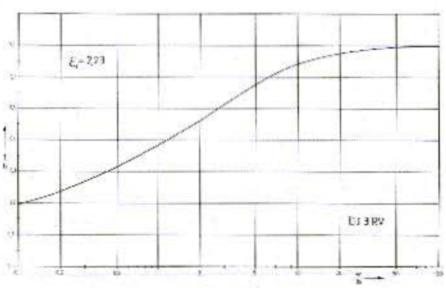

Diagram 3: Elongation of length by amount d for an open-circuited stripline for a relative permittivity of $\varepsilon_r = 2.23$

W for angles $\varphi = 30°$ to $120°$ is given. The width b is calculated from **equation (8a)**. My measurements showed that these approximations are effective for angles $\varphi = 90°$ to $120°$.

For a right-angled bend $\varphi = 90°$, the width b is determined according to /2/ also **equation (8b)**. The size of d must then be determined with **equation (7)** for an open-circuited line of width $\sqrt{2}\,W$.

The equivalent length Δl is approximately given by **equation (9)**.

4. SYMMETRICAL BRANCHING

The reference plane displacement at a line branching section is shown in **fig. 4**. This occurs with probes, conductor dividers or hybrid couplers and is extensively covered in /1/. For a symmetrical

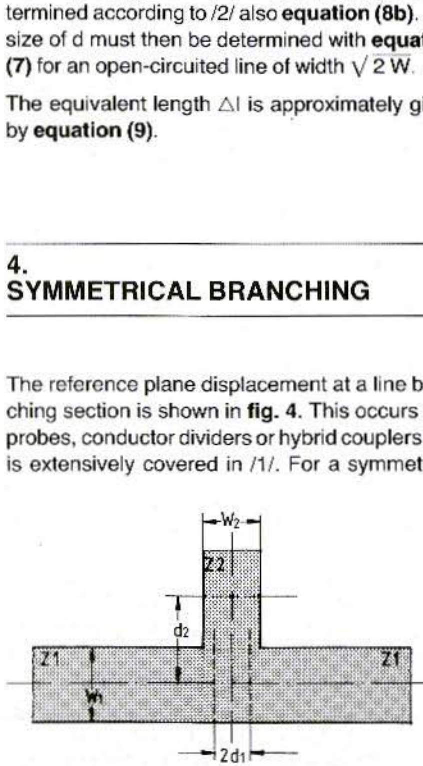

Fig. 4: Displacement of reference plane at a stripline junction

Equations:

$$\frac{W}{h} = \begin{cases} \dfrac{8}{e^{A} - 2e^{-A}} \; ; & \text{for } \frac{W}{h} \leq 2 \\[2ex] \dfrac{2}{\pi}\left[B - \ln(2B+1) + \dfrac{\varepsilon_r - 1}{2\varepsilon_r}\left(\ln B + 0{,}39 - \dfrac{0{,}6}{\varepsilon_r}\right)\right] \; ; & \text{for } \frac{W}{h} \geq 2 \end{cases} \qquad (1)$$

$$\text{where } A = \frac{Z_L}{120\Omega}\sqrt{2(\varepsilon_r + 1)} + \frac{\varepsilon_r - 1}{\varepsilon_r + 1}\left(0{,}23 + \frac{0{,}11}{\varepsilon_r}\right) \; ;$$

$$\text{and } B = \frac{60\Omega\pi^2}{Z_L \cdot \sqrt{\varepsilon_r}} - 1 \; ;$$

$$\varepsilon_{reff} = \begin{cases} \dfrac{\varepsilon_r - 1}{2} + \dfrac{\varepsilon_r - 1}{2}\left[\left(1 + 12\dfrac{h}{W}\right)^{-\frac{1}{2}} + 0{,}04\left(1 - \dfrac{W}{h}\right)^2\right] \; ; & \text{for } \frac{W}{h} \leq 1 \\[2ex] \dfrac{\varepsilon_r + 1}{2} + \dfrac{\varepsilon_r - 1}{2} \cdot \left(1 + 12\dfrac{h}{W}\right)^{-\frac{1}{2}} \; ; & \text{for } \frac{W}{h} \geq 1 \end{cases} \qquad (2)$$

$$Z_L = \begin{cases} \dfrac{60\ \Omega}{\sqrt{\varepsilon_{reff}}} \ln\left(8\dfrac{h}{W} + 0{,}25\dfrac{W}{h}\right) \; ; & \text{for } \frac{W}{h} \leq 1 \\[2ex] \dfrac{377\ \Omega}{\sqrt{\varepsilon_{reff}}}\left[\dfrac{W}{h} + 1{,}393 + 0{,}667 \cdot \ln\left(\dfrac{W}{h} + 1{,}444\right)\right]^{-1} ; & \text{for } \frac{W}{h} \geq 1 \end{cases} \qquad (3)$$

$$\varepsilon^{*}_{reff} = \varepsilon_{reff} - \frac{(\varepsilon_r - 1)t}{4{,}6\sqrt{W \cdot h}} \qquad (4)$$

$$W^{*} = \begin{cases} W + \dfrac{1{,}25 \cdot t}{\pi}\left(1 + \ln\dfrac{4\pi W}{t}\right) \; ; & \text{for } \frac{W}{h} \leq \frac{1}{2\pi} \\[2ex] W + \dfrac{1{,}25 \cdot t}{\pi}\left(1 + \ln\dfrac{2h}{t}\right) \; ; & \text{for } \frac{W}{h} \geq \frac{1}{2\pi} \end{cases} \qquad (5)$$

$$\varepsilon_{reff}(f) = \varepsilon_r - \frac{\varepsilon_r - \varepsilon_{reff}}{1 + G} \qquad (6)$$

$$\text{where } G = 0{,}168(\varepsilon_r - 1) \cdot \left(\frac{f}{\text{GHz}}\right)^2 \cdot \left(\frac{h}{\text{mm}}\right)^2 \cdot \left(\frac{Z_L}{\Omega}\right)^{-\frac{3}{2}}$$

---

junction the approximations are given in /3/ **equations (10) and (11)**. The reference plane displacement is taken from the centre lines' of the conductors. The characteristic impedance Z_1 is that of the through line and Z_2 is the impedance of the branch line. These impedances are determined with **equations (1) and (2)** or **diagrams 1 and 2** together with the relevant effective relative permittivity.

5. REFERENCES

/1/ Mehran, R.: Grundelemente des rechnergestützten Entwurfs von Mikrostreifenleitungs-Schaltungen
Verlag H. Wolff, Aachen

$$\frac{d}{h} = 0,434907\,\frac{(\varepsilon_{reff})^{0,81} + 0,26}{(\varepsilon_{reff})^{0,81} - 0,189} \cdot \frac{(\frac{W}{h})^{0,8544} + 0,236}{(\frac{W}{h})^{0,8544} + 0,87} \cdot M \quad ; \qquad (7)$$

$$\text{where} \quad M = \frac{(1-0,218e^{-7,5\frac{W}{h}})\,(1+\frac{0,5274}{(\varepsilon_{reff})^{0,9236}})\,\arctan(0,084(\frac{W}{h})^{K})}{1+0,0377(6-5\cdot e^{-0,036(\varepsilon_r-1)})\,\arctan\,(0,067(\frac{W}{h})^{1,456})} \quad ;$$

$$\text{where} \quad K = 1,9413\,(1+\frac{(\frac{W}{h})^{0,371}}{1+2,358\cdot\varepsilon_r})^{-1} \quad ;$$

$$b = W\,\frac{1-0,9\cos(\varphi/2)}{\sin(\varphi/2)} \quad ; \qquad (8a)$$

$$b = \frac{W}{\sqrt{2}} - d \qquad (8b)$$

with d from equation (7) and with width $\sqrt{2}$ W determined

---

$$\Delta\ell = \frac{h}{2}\,(0,5 \cdot (\frac{W}{h})^{1,88} - \frac{0,45}{\sqrt{\varepsilon_r}} - 0,12) \qquad (9)$$

$$d_2 = 0,5\,D_1 - \frac{D_1 Z_2}{Z_1}(0,076 + 0,2(\frac{2D_1}{\lambda})^2 + 0,663\cdot e^{(-1,71\frac{Z_1}{Z_2})} - 0,172\,\ln\frac{Z_1}{Z_2}) \qquad (10)$$

$$d_1 = 0,05D_2\,\frac{Z_1}{Z_2}\left(\frac{\sin(\frac{\pi}{2}\cdot\frac{2D_1}{\lambda}\cdot\frac{Z_1}{Z_2})}{\frac{\pi}{2}\cdot\frac{2D_1}{\lambda}\cdot\frac{Z_1}{Z_2}}\right)^2 \cdot (1-(\pi\frac{D_1-2d_2}{\lambda})^2) \qquad (11)$$

$$\text{where}\ D_1 = \frac{120\pi\Omega\cdot h}{\sqrt{\varepsilon_{reff1}}\cdot Z_1} \quad ; \quad D_2 = \frac{120\pi\Omega\cdot h}{\sqrt{\varepsilon_{reff2}}\cdot Z_2}$$

$$\lambda = \frac{c_0}{\sqrt{\varepsilon_{reff1}}\cdot f}$$

/2/ Hoffmann, R. K.: Integrierte Mikrowellenschaltungen
Springer Verlag, Berlin 1983

/3/ Hammerstad, E. O.: Equations for microstrip circuit design
Proceedings of the 5th EMC, 1975, p 268 - 272

/4/ Lieferfirma für RT/Duroid:
Mauritz GmbH & Co., Postfach 10 43 06, 2000 Hamburg 1

/5/ Lieferfirma für Di-Clad:
Municom, Postfach 12 10, 8217 Grassau

Carsten Vieland, DJ 4 GC

Power Amplifiers – How they are operated

This compilation of measures for the spurious-free operation of power amplifiers was written in the hope that it would act as a reminder and as a source of assistance, for the improvement of a few – mainly contest – stations of dubious output quality. They serve, also, as a preliminary for the accompanying article on the construction of a highly linear 750 W UHF power amplifier using a 4 CX 1000 A valve.

A power stage serves only to amplify the input signal and not to generate signals of its own. Several simultaneous conditions are to be met before a high power output together with spectral purity can be achieved:

1) The PA must be, in fact, linear.
2) The transceiver (exciter) driving signal must also have a clean spectrum.
3) When switching from exciter to PA, the transmit level must be carefully controlled – the microphone gain is unsuitable for this purpose.
4) The output must be properly monitored so that the modulation envelope can be clearly seen in operation and on a test signal – a moving-coil instrument can give a false impression.

These four conditions will be examined in more detail.

1. THE POWER AMPLIFIER

Valves and transistors used in linear power amplifiers require stable supplies in order that the working point can be fixed. These should remain, even under the most difficult input conditions, (emergency supply generators, or mobile operation). If the input envelope is influenced by signal varying DC supply potentials applied to the devices electrodes, spurious signals are generated by the non-linearity – the dreaded intermodulation. This effect is, of course, desired in mixers where an intermediate frequency is required.

Transistor power amplifiers, must therefore, have due attention paid to the base bias supply. Its stability must be checked by an oscilloscope during working conditions. For transistors having a 0.7 V bias, the input signal should not cause it to vary by more than 0.1 V peak-to-peak as a working guideline. Many commercial amateur equipments fall well short of this standard.

The screen-grid of a power valve has simular prerequisites e. g. the screen-grid of the 4 CX series should be stable within 5 V peak-to-peak under dynamic conditions. A point to watch is that, despite the required degree of stabilisation, a negative current flows over parts of the input cycle. This necessitates a large standing ballast current to be provided.

Monitoring of this voltage by means of a multimeter is not sufficient owing to its inadequate response to speech waveforms. Again, an oscilloscope is required to monitor the dynamic conditions.

Poor matching of the valve or transistor to the tuned output circuit / transformer, or perhaps poor design or mis-tuning, can also cause the production of intermodulation, despite the fact that the device is adequate for amateur output requirements.

In cases of doubt, V-MOS transistors or valves are to be preferred to bipolar transistors. At moderate modulation, using two equal input test tones, the 3rd order IM signals are some 30 dB lower but the higher orders fall away more quickly using valves. In the critical region from 5 to 20 kHz removed from the sender frequency, the level of intermodulation products could be up to 20 dB lower using V-MOS or valve PAs when compared with bipolar PAs driven to the same output and possessing the same level of IM_3.
It is well known that some valves used in the construction of PAs are simply not suitable e. g. QQE 06 / 40 and the 4 CX 250 (see test report in CQ-DL 5 / 82). The most common cause of intermodulation distortion is, unfortunately, the lack of self discipline. It is generally known that for a 1 dB increase in output power the IM_3 level can increase from at least 3 dB up to 20 dB. It would appear that attempts are made to drive the PA in order to achieve the unattainable intercept-point (roughly same level of power in speech waveform as in intermodulation products)!

2. TRANSCEIVER

The output signals of most modern transceiver are quite good and that can be confirmed by the many test reports which have appeared in the last few years. The considerations of (1) are valid, but improvements are possible in practically all equipments.

The noise side-bands of the local oscillators, however, cannot be said to be good. The output signal is superimposed, through the mixing process, upon the noise pedastal of the local oscillator. As a consequence, the low frequency modulation contains noise, which is very similar to that of intermodulation but tends to be much more broad-banded. Transceivers with unfavourable noise characteristics should never be used to drive power amplifiers, as observed in (1).

The YAESU transceiver FT 225 RD, which is considered to be really good in this respect, could be improved by 10 dB at 100 kHz from the midband signal. When a neighbouring station carried out this modification on his FT 225 RD it was then possible to work the band without mutual interference. The modification, it should be noted, is also beneficial in the receive mode.

3. CONNECTING TOGETHER EXCITER AND POWER AMPLIFIER

Even assuming that a manufacturer produces a low distortion, low noise transceiver and a good matching power amplifier, the potential exists for trouble when the two are connected together. Besides a relay contact or two for external use, the manufacturers offer nothing particularly helpful. Of notable assistance would be an HF drive control which gives continuous control over the power supplied to the PA. The microphone gain control is as much use for this purpose as a handbrake is in controlling the speed of a car. The purpose of a "mic. gain" control is to enable microphones of differing sensitivities to modulate the transceiver. Attempts to use it as a drive control could result in saturation of the high frequency audio peaks, as may be confirmed by an oscilloscope monitor. The transceiver automatic level control (ALC) counters the effect of the "mic. gain" control. The

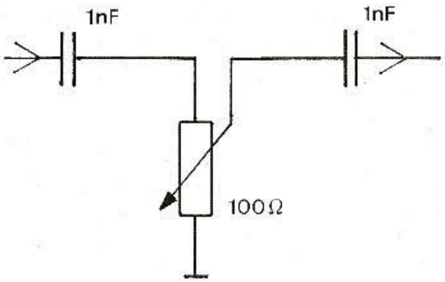

Fig. 1: Continuously variable power control inserted into a 50 Ω point in the low level RF drive circuits

application of too much ALC also causes distortion. In addition, before the ALC comes into operation, narrow impulses of up to 1 ms in duration, are produced during the time the ALC remains ineffective. These impulses have a peak power approaching that of the maximum transceiver output power, which in the case of the FT 225 RD is 40 to 50 W.

An "RF drive" control can, however, be retrofitted to most transceivers. A 50 Ω impedance point is chosen (if possible) at a low level portion of the RF amplifying chain and a suitable "blocked" 100 Ω potentiometer is inserted in the circuitry. It should be mounted at an accessible point on the equipment's front panel. The author installed the potentiometer of **fig. 1** in the 10.7 MHz IF stages of his FT 225 RD. It varies the SSB output power from zero to 25 W without other specifications being affected.

A reduction in level in the front part of the process reduces the intermodulation which would have been produced in later stages owing to overdriving. It does, however, have a somewhat adverse effect upon the dynamic compression properties of the ALC.

To complement the "RF drive" control, a vital part of the chain should be matched by constructing a suitable dimensioned 50 Ω power attenuator from composition or film resistors and include it between driver and PA. The attenuator should be dimensioned so that the PA can be driven to within 1 dB of its rated power output (**fig. 2**).

The PA cannot now be overdriven and the dynamic compression of the driver transceiver ALC remains fully in operation. The "mic. gain" is adjusted for a medium to high output level (a pointer indication may be used). A high-dynamic range receiver, monitoring the output of a local, well adjusted driver / PA combination, is able to tune within a few kHz of the transmission, without detecting appreciable spurious emissions.The attenuator between the transceiver/PA combination also serves the important role of terminating the transceiver with a real 50 Ω impedance. The IM specification of a transceiver is most favourable, when it has been terminated with a matched resistive load and thereby low return loss/VSWR. Driving a PA valve, or a transistor directly,results in a reactive load which is dependent upon the dynamic drive level.

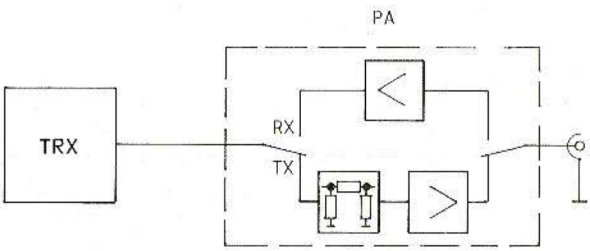

Fig. 2:
Attenuator pad inserted in the "send" arm of the PA input

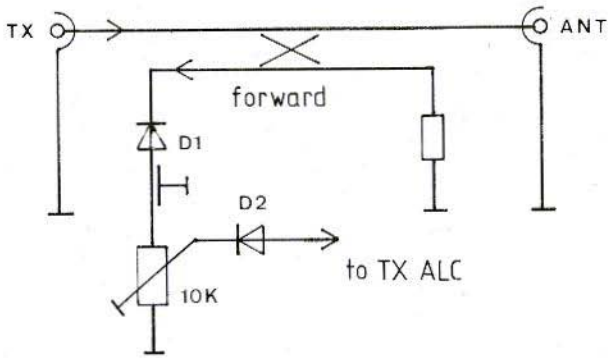

Fig. 3:
Obtaining the ALC sample voltage from the PA output

The matching from transceiver/driver into the PA via the matching pad is best carried out at full drive and output power. At lower levels the PA input impedance is far removed from the real 50 Ω. This causes a distortion of the input/output characteristic resulting in the generation of intermodulation products despite the PA output load being a resistive 50 Ω (antenna or dummy). A 5 dB pad between a 10 W transceiver and a 4 CX 250 PA can result (in a theoretically unfavourable case) in a return loss of 10 dB (i.e. SWR ≈ 2 : 1).

A further attenuation of intermodulation products is possible by taking the ALC sample from the power amplifier output and feeding it back to the transceiver with the appropriate level and time-constant to suit the equipment concerned. The circuit of **fig. 3** may be used to obtain the sample voltage, but this voltage may have to be contoured before it can be applied to the transceiver.

The power output is set to maximum by means of the 10 kΩ pre-set potentiometer. The diode D 2 output is fed to the ALC circuit in the transceiver. In some circumstances the transceiver internal ALC gain must be reduced or suppressed. Should the sample voltage be insufficient, or have the wrong polarity, it may be corrected by means of an operational amplifier.

A directional coupler is to be preferred, rather than a capacitive or inductive output tap, as it functions independently from the prevailing antenna matching conditions. The directional voltage can also be used for an accurate power output indicator.

4. OUTPUT MODULATION MONITORING

The transmitted signal from the transceiver / PA equipment must be monitored under all working conditions all the time. Moving-coil instruments give a false indication because with speech only average fluctuations may be shown and never the peak values. The only effective form of monitoring the output of a high power transmitter under working (traffic) conditions is to use a simple DC oscilloscope.

The individual workings of measures designed to produce the optimum conditioning for the transmitted audio, such as ALC, high AF attenuation and speech-processing, have the combined effect of concentrating the power into the middle dynamic range, thereby increasing its average

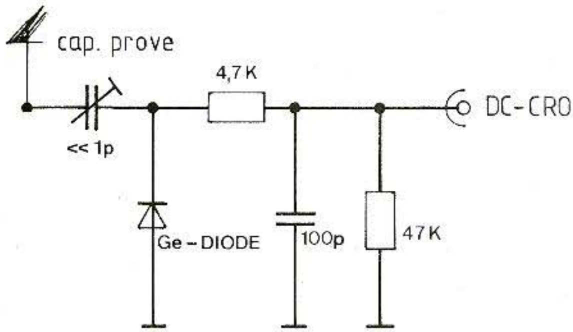

Fig. 4:
Envelope detector with a high video frequency

value. The peak values, on the other hand, do not reach saturation. The optimisation during tuning, adjustment and operation is expeditiously carried out whilst observing the transmitted signal's modulation envelope. Some radio amateurs would have the cause of annoying splatter and speech distortion, right before their eyes.

A particularly good indicator for linearity and output is facilitated by the two-tone test, as this encompasses nearly all aspects of the output performance, it can be used for optimising individual stages during tune-up. Experience has shown, that a 3rd order intermodulation of – 30 dB relative max. output power can be expected, if the monitor trace shows no visible departures from the ideal detected two-tone pattern. For a suitable trace, the demodulation should be effected with a short filter time-constant in order that the signal is not distorted. The demodulator should also be capable of handling video signals of at least 50 kHz. The sample signal must be much greater than the diode barrier voltage. Greater than 3 V is required in order to prevent distortion from this cause. The detector probe must be adjusted to the HF pick-up point until a satisfactory level has been achieved. A suitable detector is shown in **fig. 4** for PAs without a reflectometer.

Most commercial PAs have a demodulated HF monitor already built-in but it must be modified normally, in order to reduce the detector time constant.

To faithfully reproduce the two-tone RF envelope, the diode capacitor should be reduced to about 100 pF and the diode load to about 10 kΩ.

5. REFERENCES

(1) Leif Åsbrink, SM 5 BSZ
Dynamie Range of 2 m Transceivers
VHF-COMMUNICATION Vol. 14
Ed. 1 / 82 P. 49 - 55

(2) Günter Schwarzbeck, DL 1 BU
Endstufen für das 2-m-Band
CQ-DL Heft 5 / 82

(3) Günter Schwarzbeck, DL 1 BU
Geräte-Eigenschaften bei SSB und CW
Besonderheiten zwischen Testbericht und Praxis
CQ-DL Heft 9 / 82

(4) Gühter Schwarzbeck, DL 1 BU
Testbericht VHF Hochleistungsendstufe mit 4 CX 350
CQ-DL Heft 2 / 81

(5) Thomas Molière, DL 7 AV
Der Stationsmonitor SM 220;
Testbericht und Meßdaten
CQ-DL Heft 6 / 81

(6) Wolfgang Günter, DF 4 UW
Linearendstufen-Übersteuerung
CQ-DL Heft 4 / 81

(7) Dr. Richard Waxweiler, DJ 7 VD
Niederfrequenz-Zweitongenerator
CQ-DL Heft 8 / 81

(8) Günter Schwarzbeck, DL 1 BU
SSB-QRM
CQ-DL Heft 7 / 75

Carsten Vieland, DJ 4 GC

Two-metre Power Amplifier using Valve 4 CX 1000 A

A two-metre power amplifier will be described which will deliver a power output of 750 W with a high spectral purity. As the construction of such an amplifier requires skill, experience and patience, I would rather not repeat to experts the various circuit techniques but confine my comments to the peculiarities of this particular valve. The intermodulation free, i. e. splatter free, operation should also be extended to its use as a mobile PA where the construction of the power supply will merit particular attention owing to the strongly varying voltages encountered.

Contrary to longstanding opinion, the ubiquitous valve family 4 x 150 / 4 CX 250 were not made for linear operation but for class C AM and FM applications some forty years ago. The tetrode 4 CX 1000 A / JAN 8186 (**fig. 1**), on the other hand, was especially developed for SSB and television linear amplification over a wide dynamic modulation range. It is not, unfortunately, quite as robust as its smaller predecessors and requires greater care both in construction and operation.

The CX 1000 A is a beam tetrode i. e. the screen-grid lies directly in the shadow of the control grid. This calls for great precision during its manufac-

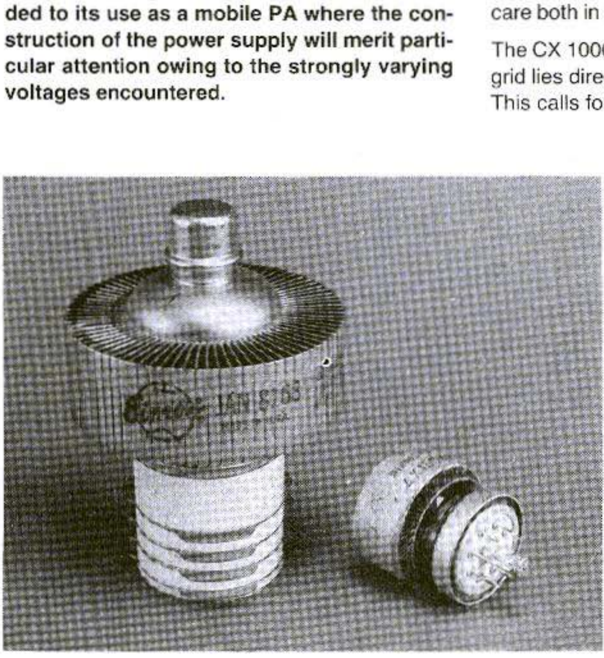

Fig. 1: The 4 CX 1000 A or JAN 8186

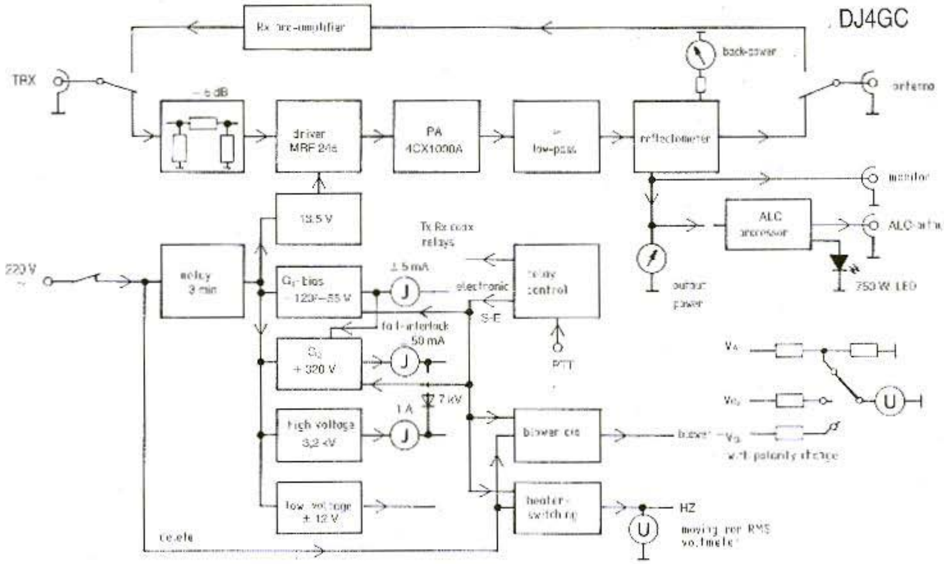

Fig. 2: Final with penultimate block diagram

ture and during its operation, great care must be exercised to ensure that even a transient overload does not occur which could lead to buckling and misalignment of the beam structure. The manufacturers specify a permitted control-grid power dissipation of zero watts. Nevertheless, a peak value of 5 mA occasioned during modulation may be allowed. In the course of the years I have tested a number of tubes (including original-packed) that have differing characteristics under working conditions. It gives the impression of a certain "overbreeding".

1. CIRCUIT DESCRIPTION

The overall function may be determined from the block diagram of **fig. 2**. The actual amplifying stage is also given in the detailed schematic of **fig. 3**. According to the manufacturer Eimac, the maximum frequency of the 4 CX 1000 A using the original socket SK 800 lies around 110 MHz. The version 4 CX 1000 K has a maximum working frequency of 400 MHz although both tubes have identical connections and use the same socket. The airvent holes on the screen grid plate of the socket SK 800 should , through screwed on tinplate, be covered just sufficiently to allow the tube to be changed. After this modification the 4 CX 1000 A is suitable for use up to 145 MHz. The airblast from the 80 to 100 W blower is directed into the anode and then through a teflon or drawing-cardboard cylinder to the exterior of the enclosure.

The screen-grid blocking condenser (5 nF), which is integrated into the socket, is insufficient to prevent spurious oscillations. This is manifest upon switch-on by a self-oscillation in the long-wave region caused by the screen-grid choke forming part of a resonant circuit. It may be cured by a

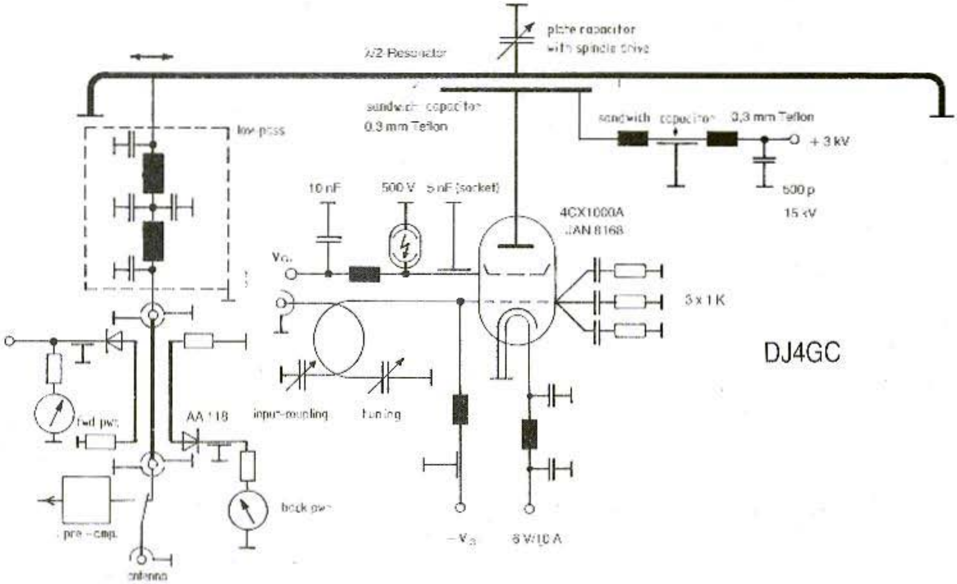

Fig. 3: Schematic of PA stage

dampend choke of, at most, 10 μH and a further capacitor of 10 nF. In order to avoid noise in "stand-by", the screen-grid is switched to ground. The filter capacitors must not be too large in order that the relay contacts do not have to switch an unnecessarily large charge current.

As the screen-grid current, in operation, is negative owing to secondary emmission, it should be loaded to earth by at least 70 mA of bleed current. The screen-grid line, with its components, is also protected from voltage surges by a 400 - 600 V, gas filled, surge-arrester.

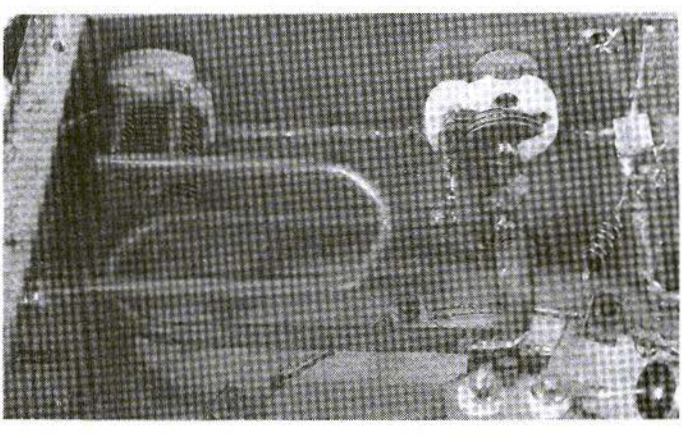

Fig. 4: Constructional details of grid circuit and input coupling

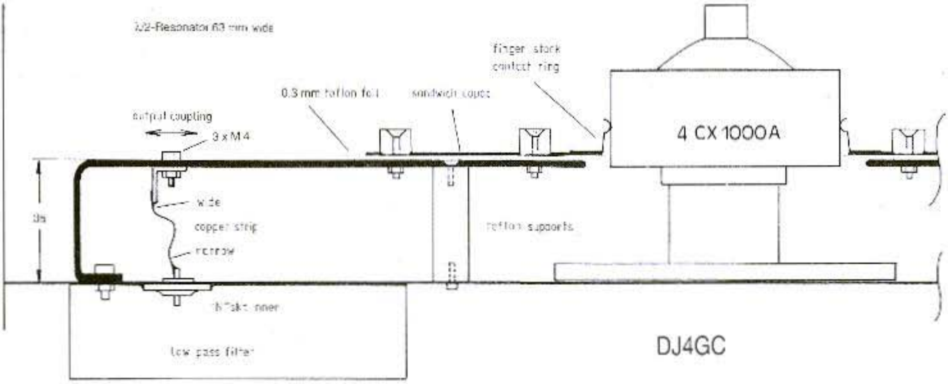

Fig. 5: Constructional details of anode tuned circuit and output coupling

The valve has a high transconductance of 30 mA / Volt and therefore a high grid-cathode capacitance of about 90 pF. A λ / 4 tuned-circuit cannot be used, as the voltage-node will be produced rigth at the socket. A favourable solution turned out to be a λ / 2 tuned circuit which is tuned at the opposite end of the valve. The drive input is coupled inductively, a further variable capacitor compensating the total inductance in the grid lead (**fig. 4**).

Each of the three control-grid connections of the socket is taken to a 1 kΩ resistor via blocking capacitor thus forming a parasitic stopper which effectively dampens any tendency to oscillate at low frequencies. They have little effect upon the wanted signal as at this frequency the resistors lie at a voltage node. The geometry and coupling of the tuned circuit must be optimised experimentally.

The valve's anode tuned circuit has a diameter of 85 mm. In order to avoid transittime effects and to equalise the current distribution, the resonant circuit should load the anode uniformly at all points. After a few abortive attempts, an optimal solution turned out to be a 65 mm wide, λ / 2 conductor tuned-circuit with the anode in the middle of a current anti-node and a direct output coupling (**fig. 5**). The anode supply voltage is introduced at the cold end of a plate (sandwich) capacitor. The resonator itself is connected to ground as far as DC is concerned. The valve anode is connected to the coupling capacitor by means of contact-finger stock. The coupling capacitor itself is formed by sandwiching a 0.3 mm teflon sheet between capacitor and resonator surfaces, using teflon and ceramic supports. As the anode potential climbs to 4 kV when the amplifier is quiescent, it is important to ensure that the construction of these parts allow no chance for ionized paths to occur between fixing-screws and the capacitor. The teflon supports are therefore so recessed that they protrude 0.1 mm beyond the thickness of the capacitor plate. Two further teflon supports hold the resonator at a constant level above the chassis. The output tuned circuit is so stable that even after a long period of operation it does not require retuning. The circuit is brought to resonance by a tin-plate disc, earthed by a flexible braid and tuned by a spindle drive.

The output coupling lies about 60 mm from the "cold" end of the tuned circuit. The contacts are made by a brass angle piece secured with three screws. Its position is adjustable over a few centimetres in order to effect a correct output match (**fig. 6**). A low inductance length of braid, or copper-foil, is soldered to the angle-piece and the

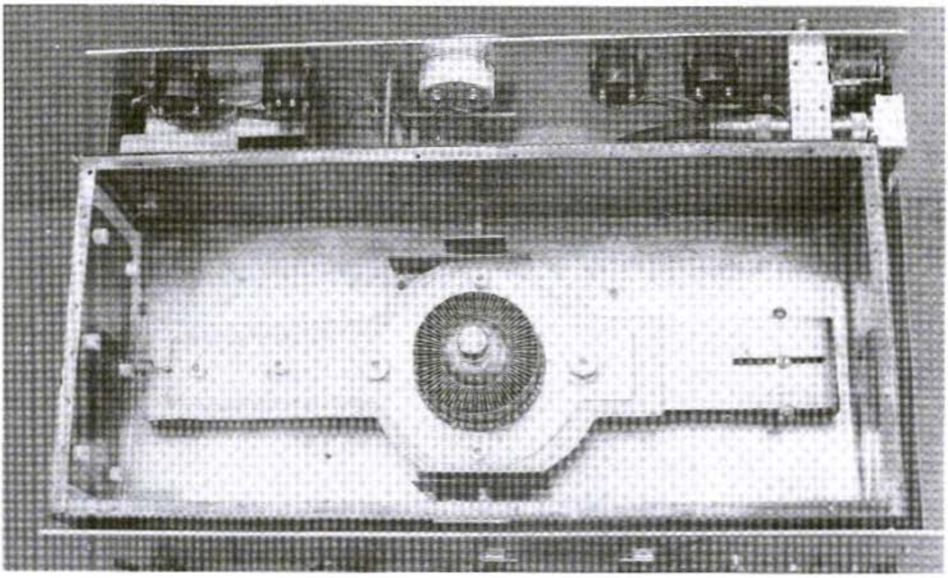

Fig. 6: Overall view of output circuit with top cover removed

orther end is connected to a feedthrough point which consists of the teflon-supported, inside conductor of an N-socket.

Under the resonator floor, a two-stage low pass filter is situated which is housed in a 50 mm high commercial tin-plate box. With the high-quality air-spaced trimmers, which were ready to hand, the frequency limit was 200 MHz. Instead of the expected attenuation, there was a slight increase in power after the reactive element was tuned out of the output line by the trim-capacitors.

The output is then taken to a reflectometer via "N" connectors. Antennas with a returnloss of more than 15 dB (SWR 1 : 1.5) should not be used owing to the high level of RF introduced into the station via the high coaxial-screen currents. For this reason, two separate meters showing both forward and return power are built into the PA.

From the reflectometer forward-coupler, a sample is extracted for the automatic level control (ALC) which is prepared and fed back to the external driver (transceiver) see **fig. 7**. A red LED illuminates when the maximum permitted output power of 750 W has been exceeded. By means of the ALC, or a carefully adjusted speech processor, this limit should be difficult to attain during operation.

The forward voltage of the directional coupler is taken to a monitor output in order that the operation may be constantly monitored with a simple DC oscilloscope (CRO). This simple method of monitoring should be noted by all high power stations, as the use of a pointer instrument for this purpose is totally inadequate because of its slow response to audio. Contests, in particular, seem to be accompanied by intermodulation splatter all too frequently.

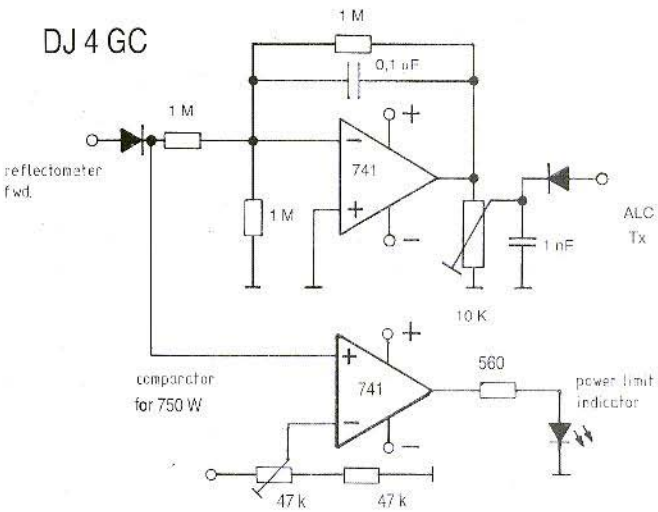

Fig. 7:
The ALC processing circuits from the directional coupler forward port

The power gain of the 4 CX 1000 A is not very high on account of its low input impedance. An input of 10 W is necessary for an output power of 750 W. The input impedance also, is dependent upon the signal and is only 50 Ω resistive at one pre-determined optimised output power. This optimising is best carried out at peak output for SSB operation. Unfortunately, on the German market, there is hardly a transceiver to be found which is capable of delivering an acceptable quality ($IM_3 > 30$ dB) to a dynamic load (i. e. an independance which varies with the signal). A driver stage was therefore included in the PA, which was operated at well below its 1 dB compression point. The 12 V transistor MRF 245 used for this purpose, caused no appreciable distortion to the transceiver.

The gain of this penultimate driver stage was measured at 11 dB. The transceiver power was reduced 5 dB by including an attenuator pad before the transistor driver. This measure serves both to improve the dynamic load to the transceiver and to reduce the level of return-loss on the transceiver / PA coaxial cable.

2. POWER SUPPLY

The power supply for a two-stage power amplifier is somewhat involved but the extra effort ensures that the PA will behave properly under all signal conditions and also when using mobile power supplies. Even so, the HT voltage varies by some 40 V_{RMS} between extremes of signal, despite its internal regulation. Special problems were caused by the waveform of this supply voltage. During no-signal conditions pulses occurred which had a peak of 2.8 kV rising to a horrendous 4.4 kV under full load conditions despite using a low-ohm, over-rated, laminated transformer. The complete HV side was tested with a 6.5 kV generator. All sharp edges were rounded in order to avoid corona discharges. These discharges were made, manifest as small blue sparks which not only pressaged a full scale arc-over but also caused severe noise side-bands to be generated.

The HV transformer was connected to the mains via a bridgeable 10 Ω protection resistor.

The high voltage filtering is carried out by a chain of electrolytic capacitors with a nominal voltage of 6.5 kV. The total capacitance was about 70 μF. With this arrangement, care should be taken that identical, newly manufactured capacitors are used. Also, before use, all electrolytics should be "reformed" up to their rated voltage. In order to distribute the voltage equally across each capacitor and also to act as a protective bleeder, each capacitor was shunted with 220 kΩ. The potcapacitors were mounted upon an insulated plate. The power supply enclosure was ventilated by a small, low profile fan in order to prevent the build-up of warm areas.

The screen voltages is 320 V and stabilisation is mandatory. Owing to the large variation of the input voltage 400 - 600 V on mobile, a zener stabilised supply is hardly possible because of the high heat loss both in the diodes and their dropping resistors. The efficiency of a zener stabilised supply is also, not particularly good.

The stabilisation method eventually employed, was that typically used at low voltages (**fig. 8**). This requires a careful selection of the series-pass transistors to ensure that, at small current loads, the current amplification factor lies partly under unity. At the time of the construction, there were no favourably priced, high voltage MOS-FETs which would serve the purpose. The 1N-4007 diode in the screen-supply, guards against damage to the electronics in the event of the screen-grid going highly positive as a result of secondary emission in the valve.

The control-grid voltage was adjusted in order that the anode quiescent current was 200 mA and this occurred at a bias of - 60 V (approx.). When switched to "receive", this bias is increased to − 120 V, the adjustable voltage stabilisation being quite conventional.

A particular point to mention concerns the filament power. The manufacturer specifies a maximum RMS variation of ± 5 % which cannot be achieved (at least without some complication) under mobile conditions. Using a normal 230 VAC mains input there is of course, no difference between send and receive filament voltage but the problem arises when the filament transformer input is derived from mobile sources. As the DC stabilisation at 6 V / 10 A is costly in terms of both power consumed and circuit complexity, it was

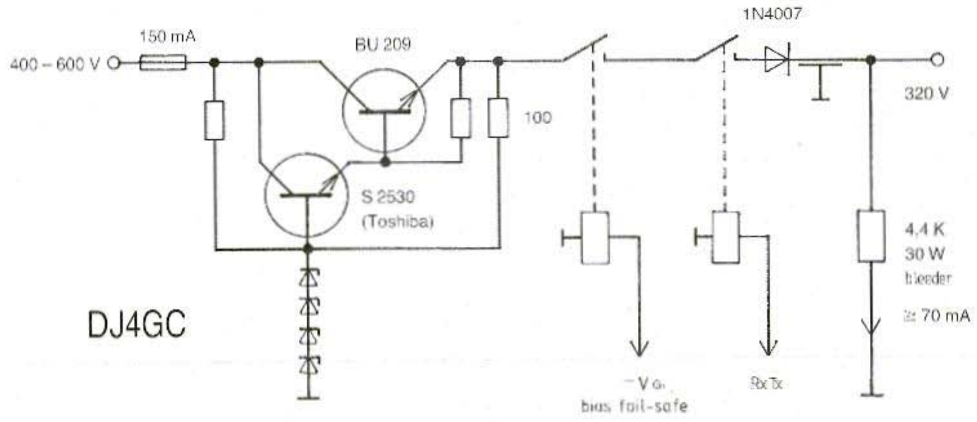

Fig. 8: Screen-grid power supply

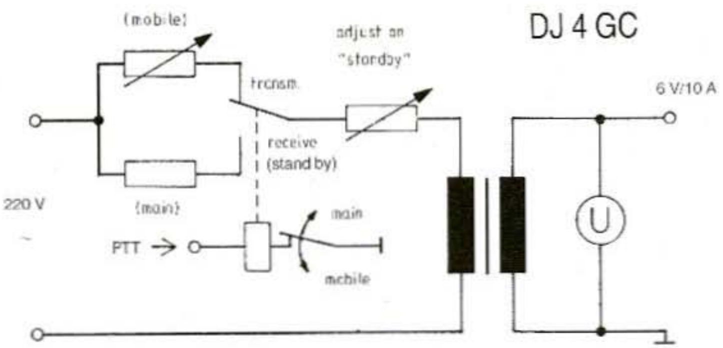

Fig. 9: Filament heating arrangements

decided to control the filament in two adjustable stages upon operation of the PTT switch (**fig. 9**). The heater voltage is adjusted to exactly the right amount, as shown on an external moving-iron voltmeter, on "receive". By this means, the voltage is prevented from exceeding the limits in the receive condition. In mobile operation adjustment of the wire-wound potentiometer RV is carried out under medium modulation conditions, the filament voltage being adjusted to an average of 6 V. The thermal inertia averages out the variations in heating power. In order to reduce the switching current, these filament stabilisation measures are effected in the transformer primary. The transformer itself, is rated at 7.5 V / 10 A.

The air-blower for the PA valve can be switched during "receive" conditions to a lower revolution rate by means of a switched resistor in its mains supply as in **fig. 10**. The power rating of this resistor may be reduced by shunting the motor with a capacitor of 2.2 μF thereby also protecting the relay contact. In the "receive" mode, the blower is so silent that it is unobtrusive.

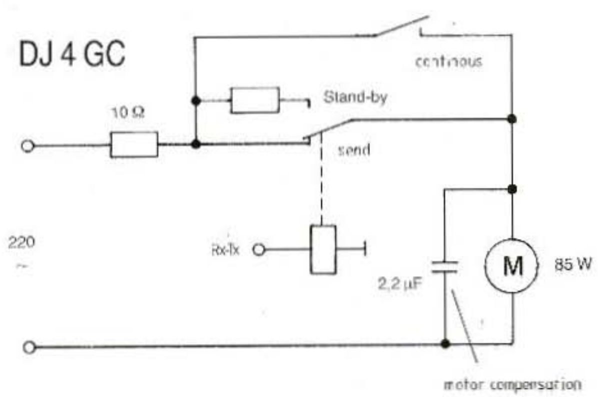

Fig. 10: Blower send / receive switching

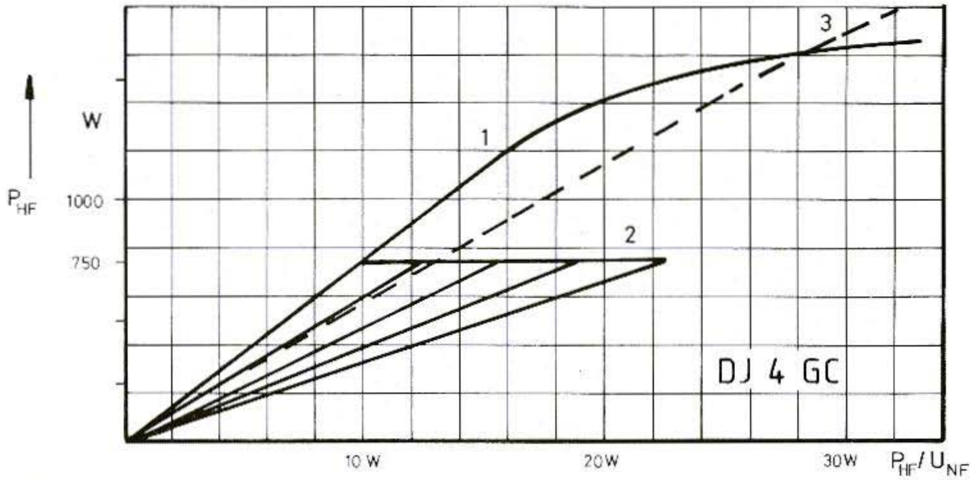

Fig. 11: PA output characteristic

3. MEASUREMENT DATA

The indicated amount of output power and control power is provided by the directional coupler of which both the forward and return coupling losses are accurately known. The indicators are two thermal power-meters. The power output (**fig. 11**) concurs most favourably with other methods of measurement.

Curve 1 indicates the adjustment optimised for a power output of 750 W. It will be noticed, that the characteristic is still linear at powers far in excess of the maximum permissible limit. The absence of kinks and bends in the characteristic, denotes the use of a valve which has been expressly designed for linear operation. Modulation by a single tone shows a sharp saturation at 750 W owing to the influence of the ALC (curve 2). Speech modulation reduces the system gain, according to the time-constant of the automatic level control so much, that only the peaks are allowed to attain the rated output. The triangular shaped area within curve 2 indicates the range of control of the ALC. Curve 3 shows the amplifier adjusted under HF drive conditions to full output where the 1-dB compression point occurs at 2 kV. The anode voltage is 3.2 kV and the quiescent current 200 mA.

A particularly revealing test of the amplifier's linearity was made with the two-tone test. The usual two-tone test, carried out with two audio applied tones and described in many test reports, was not employed. This test is an overall system evaluation as the low frequency and translation stages within the exciter / transceiver are also tested along with the intended subject, the PA alone. A spectrum analyser of sufficient resolution ($\leq$ 100 Hz) was not available in any case. The two-tone test was therefore carried out at the signal frequency using two signals of the requisite power and separated by 10 kHz from each other. The mutual coupling between the test signals was better than 30 dB rel. TT level. The two senders employed for this purpose were, an IC 202 (amplified) and an FT 225 RD. They were combined by means of a 3 dB loss, combiner transformer.

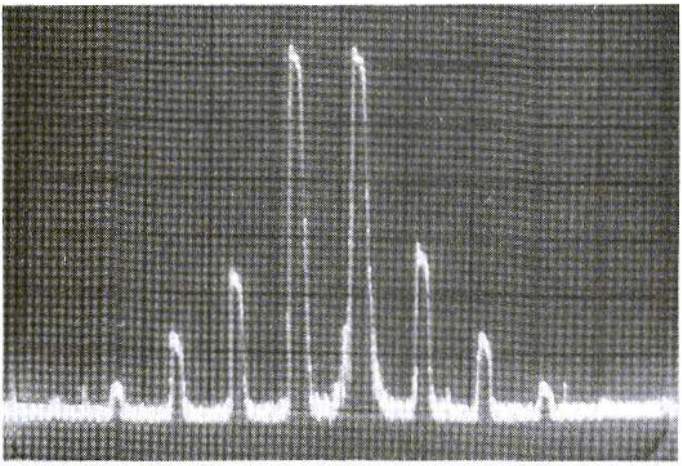

Fig. 12: Intermodulation spectrum for 2 x 188 W output power (750 W peak power) $I_{G1} = 0$ mA h: 10 kHz / box v: 10 dB / box

Fig. 12 shows the output spectrum with each signal frequency at 188 W. This is equivalent to a signal driving the amplifier to 750 W peak output power. It can be seen immediately, that the third order intermodulation side frequencies are 34 dB and 39 dB, right and left resp., relative to the level of one of the test signals. Taking the 6 dB greater peak power as a reference, the IM_3 spurious are then 40 and 45 dB down respectively. The level of the higher order intermodulation products fall rapidly with increasing distance from the two signals. The production of unbalanced IM_3 products is caused by unequal coupling losses from one output branch to the other in the combiner transformer.

The next measurement was carried out with the transistor MRF 245 driver stage included and the two-signal senders suitably attenuated. The IM_3

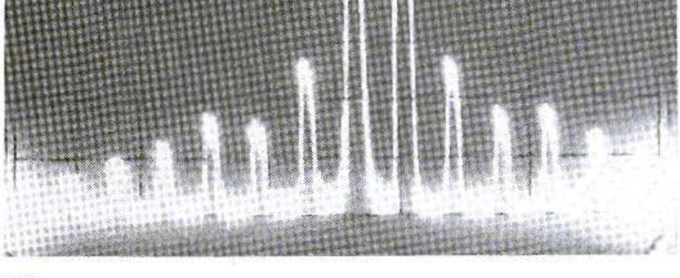

Fig. 13: Intermodulation spectrum for 2 x 188 W output power including MRF 245 driver stage h: 10 kHz / box v: 10 dB / box

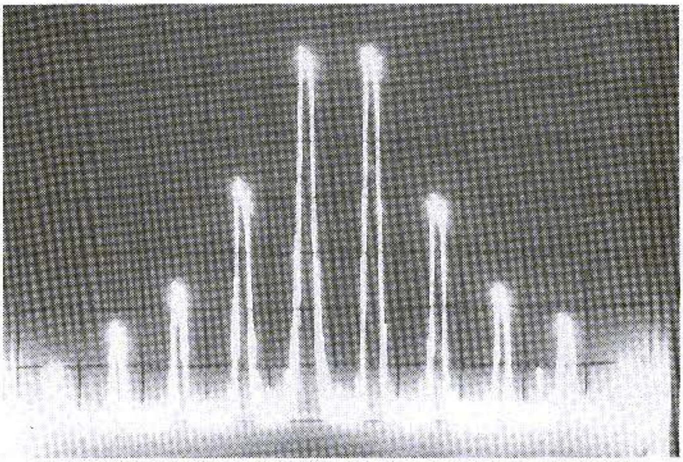

Fig. 14: Intermodulation spectrum for 2 x 500 W power output (2 kW peak)
$I_{G1} = -1.4$ mA
h: 10 kHz / box
v: 10 dB / box

result remained similar to that of the first test as can be seen in **fig. 13**. The higher order intermodulation products however, do not fall away quite as quickly – a characteristic which is peculiar to transistor amplifiers. Since it is the higher order IM products which are responsible for splatter interference to adjacent channel stations, the use of an over-rated power transistor for the penultimate driver stage, was well justified.

Another point to be observed from these analyser oscillograms is the differing degree of carrie noise on each sender used for the test. Although the FT 225 RD is considered to be good in this respect, the higher reputation enjoyed by the IC 202 (VXO local oscillator) is well justified. The latter is the lower of the two test signals in **fig. 12**.

The high linearity and dynamic range of the valve

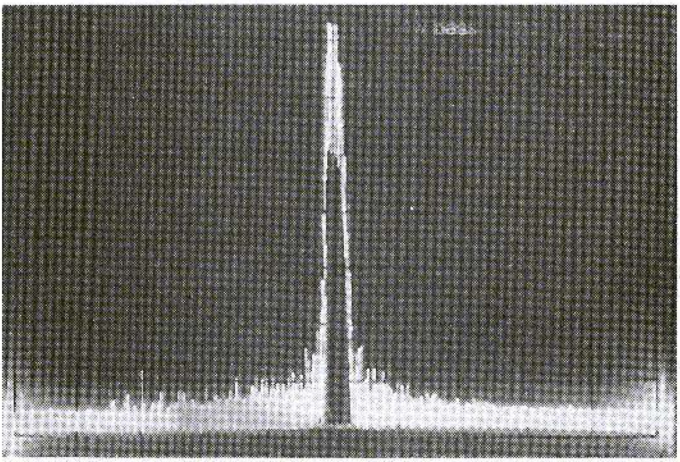

Fig. 15: Modulation spectrum of a spoken "A" driving amplifier to 750 W peak output
h: 10 kHz / box
v: 10 dB / box

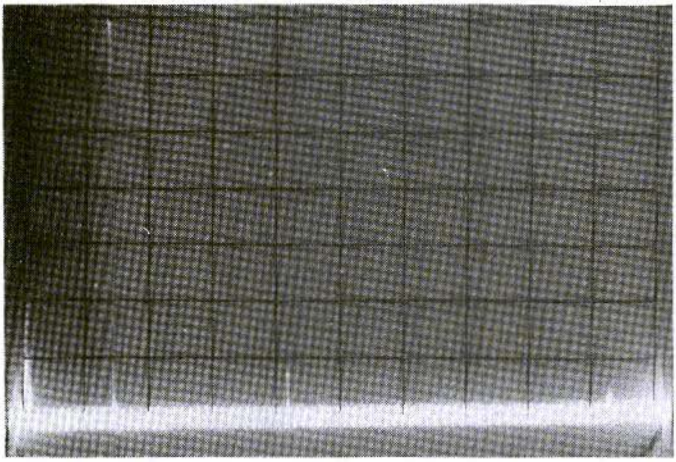

Fig. 16:
Harmonic spectrum over range 0 to 1000 MHz with single tone 750 W output
h: 100 MHz / box
v: 10 dB / box

can be seen in **fig. 14** where the amplifier has been driven to an output of 500 W for each tone, i. e. a total of 1 kW. The rapid decline of the intermodulation products testify to the very large reserve that the amplifier has, when working at its rated output of 750 W peak and to its outstandingly clean output signal.

A very appropriate test, which displays the amplifier's ability to produce a clean signal under actual traffic conditions, is shown in **fig. 15**. The FT 225 RD driver and the subject PA was modulated by voice – a prolonged "A". The peak power was 750 W but the bandwidth, taken between the level of – 60 dB products, was only ± 5 kHz!

The harmonic spectrum is displayed in **fig. 16** for an output signal of 750 W. As an attenuator for this power was not available, the monitor signal was taken from a directional coupler. This presents a rather more pessimistic display than is merited, because the directional coupler has a 16 dB falling coupling-loss to 1000 MHz and at 430 MHz the displayed third harmonic is 10 dB higher than it actually is. The confusion of light at the extreme right-hand of this trace was not caused by a signal. The extreme spectral purity of the output signal testifies, not only to the linearity of the valve, but also to the high Q of the output low pass filters.

4. OPERATING EXPERIENCE

The amplifier, as described in this article, has been in use for some four years now. Faults have been confined to changing two valves which showed a tendency to internal arcing. This occurred despite pre-heating them for several days before operation.
On account of its sensitive grid structure and employment at high powers, this type of valve is far more endangered by incorrect operating conditions than its smaller brothers. At the same time, a high degree of linearity is attained with it. Despite the close proximity of two-metre stations in the populous Ruhr area, there has been problems only in extreme vicinity of the signal pass-band, as even 80 dB suppressed spurs can cause trouble to adjacent channel stations.

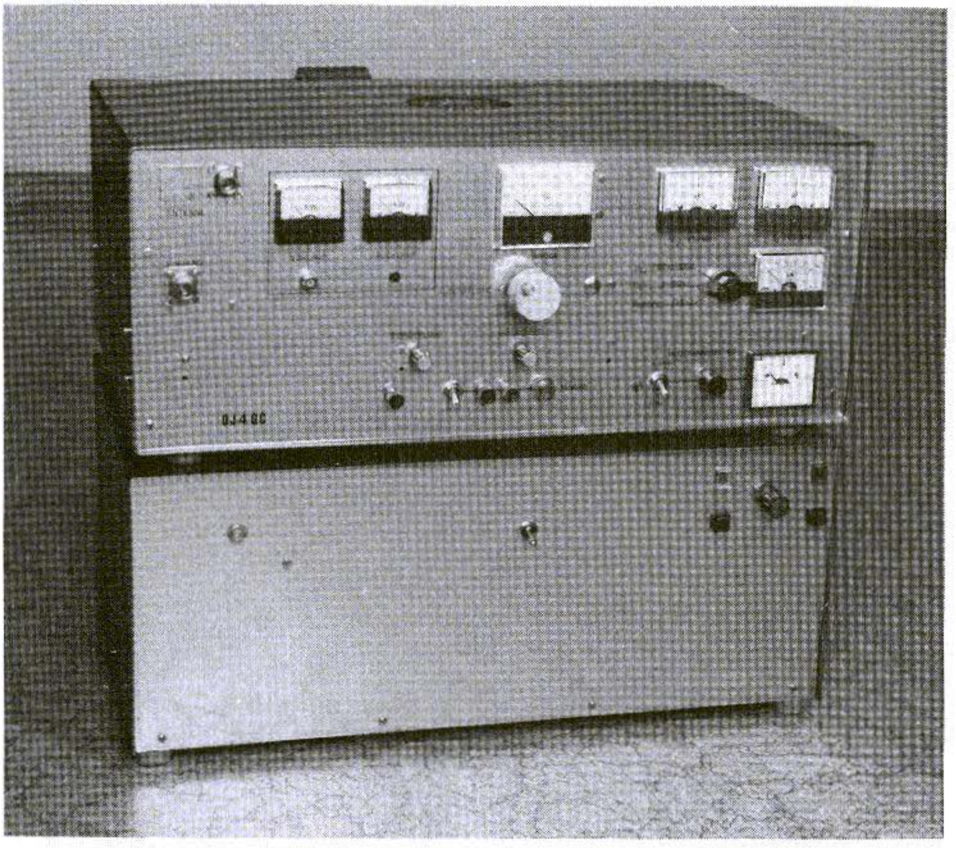

Fig. 17: Power amplifier with power supply.
The blower intake be seen at the rear and the output vent in the topcover.

Most stations are equipped with receivers having MOS-FET mixers and add-on GaAs-FET pre-amplifiers – a combination that can easily be overloaded. The use of a PLL also sets a limit to a receiver's dynamic range due to increased local oscillator phase-noise. This applies especially to the older generation of PLL oscillators. The use of a clean and powerful final stage is only one component of a successful station, other flanking measures include the station receiver, the antenna and TV-owning neighbours. Many operators under contest conditions seem to call (endlessly) as a modus operendi. Under the assumption that they all possess a spectrally clean signal, many more stations can use the same limited band for DX contest working.

The operation of such a powerful final stage requires the upholding of a few conditions:

1) The readiness to accept the high technical cost in exchange for superior linearity.

2) In operation, a constant monitoring on an oscilloscope, of the modulation envelope.

3) Never to exceed the statutory power output.

4) Self discipline under operating conditions – never use the power available to "elbow your way in" – other stations want to work DX too.

The completed power amplifier and power supply is shown in the photograph of **fig. 17**. Its construction should not be undertaken lightly, or carried out half-heartedly, but in a spirit of learning whilst constructing with the aim, always in mind, to create a quality linear power amplifier. It should also be mentioned, that very few of the components will be ready-to-hand for most amateurs and therefore many expensive components must be specially purchased.

The problems and snags encountered can be only briefly mentioned here. A project of this complexity requires individual ingenuity and optimisation and that is the reason why this article is not written like a cooking recipe. Insufficient experience in construction techniques, or in the use of test instruments, can result in a very expensive failure.

5. LITERATURE

(1) Eimac:
Data for tube 4 CX 1000 A / JAN 8186

(2) The Radio Amateur's Handbook (ARRL)
"VHF- and UHF-Transmitting" over several years
a) A 2-kW PEP Amplifier for 50 to 54 MHz
b) A 2-kW PEP Amplifier for 144 MHz
c) A 220 MHz High-Power Amplifier

Erich Stadler, DG 7 GK

Behaviour of Reflected Pulses along Cables

Sine waves and pulses have similar propagation and reflection behaviour along cables. The phenomenon of total reflection and of matching of pulses is perhaps better understood by using the mechanical analog of perturbations along a length of rope. Also, the calculation of reflection coefficient with ohmic loads, is easier to explain with pulses than with sine-wave energy. The electrical process at relatively low frequencies and long propagation times is demonstrated more simply with a sufficiently long cable.

1. TOTAL REFLECTION AND MATCHING USING A MECHANICAL MODEL

A mechanical impulse is caused on a length of rope by the means shown in **fig. 1**, where the hammer may be regarded as a pulse generator. The pulse travels, from left to rigth, down the line until its end. What happens then is determined by three cases:

a) The rope is tied to an immovable object (fig. 1 a):

The pulse will be reflected at the rope's end with the same amplitude but at the opposite polarity to that of the incident wave. The end is anchored to an immovable object; therefore, no energy can be imparted and the incident energy is reflected in its entirety. The polarity change is brought about because the incident and reflected waves simply cannot exist together at the same time because the rope's end is tied to an immovable object.

b) The end of the rope is free (fig. 1 b):

The end of the rope is free inasmuch that it is held in position by a very much thinner length of cotton, which allows the rope's end to move when subjected to a mechanical stimulus. The perturbation travels down the rope, and again, is reflected in its entirety but as the end of the rope is free to assume any position, the reflected wave has the same polarity as the incident wave. The wave is totally reflected as in the first case but if a high-speed photograph was taken at the moment the incident pulse reached the end of the rope, it would show that the end flies up to a position which is twice that of the amplitude of the incident pulse. This indicates that at this instant the total

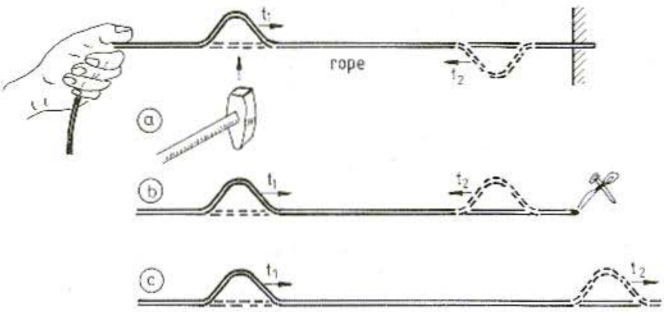

Fig. 1:
Propagation of pulses along a rope,
a) fixed end,
b) loose end
c) Rope infinately long

amplitude consists of the sum of both the incident and the reflected pulses as they overlap.

c) The rope is fastened in a medium (fig. 1 c):
The medium is considered to be so pliable that all the energy in the pulse is dissipated as heat. In this case, no energy can be reflected at all. The same effect would occur if the rope were infinately long. The impulse would travel on and on until it lost all its energy in frictional heat. Reflected waves cannot occur. In the electrical analogy it is called a "matched" condition.

2. TOTAL REFLECTION AND MATCHING USING CABLES

The mechanical analogy will now be dispensed with by using a cable instead of a rope and an electrical square wave generator instead of a hammer. This may be seen in the series represented in **fig. 2**. The **"fixed end"** here is shown in

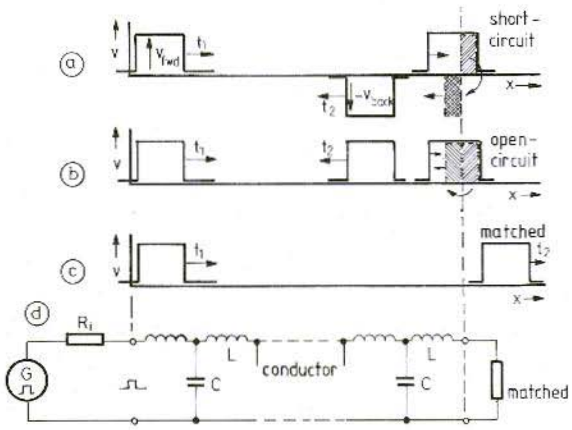

Fig. 2:
Propagation of pulses along a lossless conductor
a) short-circuited
b) open-circuited
c) matched
d) equivalent circuit of a conductor

fig. 2 a and is represented by a short-circuited cable-end. At a short-circuit, no voltage exists across it (voltage node). This has the effect that the incident pulse develops a voltage which is of the same amplitude but of opposite phase. Since it is at the end of the line, the pulse has no option but to travel, with reversed phase, back down the line from whence it came. The returning wave transports, a practically reactive power, back into the generator. If the generator is not matched to the cable, the pulse will be reflected again, this time by the generator's internal impedance.

Fig. 2 b shows the case of the **"loose"** or **"open-ended"** line. Ignoring the possibility of radiation from the cable end, it may be seen that no energy can be dissipated in an open-circuit. At the open end of the cable the pulse can develop until it has the same amplitude and phase as the incident pulse. At the moment of encountering the open-circuit the instantaneous voltages rise to double that of the incident pulse alone. This can easily be seen with the aid of an oscilloscope. This doubled voltage corresponds to that of the generator when open-circuited. Along the line, each individual input has an amplitude of half that of the generator open-circuit voltage (assuming that the generator output resistance R_i is the same as the characteristic impedance Z_o of the cable).

The **"matched case"** is shown in **fig. 2 c**, which means in this, the electrical analogy, that at the end of the line the pulse finds the same conditions of voltage and current as was encountered along the whole length of the line. The relationship between voltage and current on the line is determined by its inductance and capacitance and is of the form $\sqrt{L/C}$. This is also an expression for the characteristic impedance of the cable Z_o and if it is equal in value to the load resistor $Z_o = \sqrt{L/C} = R_L$ then all the power in the pulse will be dissipated in this load termination at the end of the cable. This is analogous to the mechanical case of the infinately long rope. The electrical energy of the travelling pulse would eventually disappear in heating the small, but ubiquitous, copper and dielectric loss resistances along the line.

In **Figs. 2 a** and **2 b** the hatched areas at the cable end show how the reflected impulse development may be imagined. The incident pulse just cannot grow out of the end of the cable. The projecting piece x can be regarded as folding back upon itself in the open-circuited case and also in the short-circuited case but this time with an inverted polarity. The superimposition of incident and return impulses, is however, not shown in fig. 2. This voltage doubling be observed on an oscilloscope by monitoring a point along the line where a reflected pulse meets the next incident pulse in the pulse train sequence.

2.1. Partial Reflection

It is plausible that between the extremes of short-circuit and open-circuit there will be a case of partial reflection. If at a point along the line there is a discontinuity causing a reflection, the point is known as a "line fault". Only a fraction will continue down the line and another fraction is returned to the generator. The same sort of thing occurs when the line is terminated by a load resistance. The load resistance dissipates part of the energy as heat and reflects the rest back towards the generator, the amplitude being smaller than that of total reflection. This condition is known as a "mismatch". The mismatch can tend towards being a short-circuit or it can tend towards being an open-circuit according to whether the termination is less than Z_o or greater than Z_o respectively. The relationship between the amplitude of the return pulse to that of the incident pulse is known as the "reflection coefficient" (**fig. 3**).

2.2. Example

A pulse generator, internal impedance $R_i = 50\ \Omega$, has an unterminated output voltage $\hat{V}_o = 20$ V. A resistive load of 75 Ω is connected to it via a length of "lossless" cable having a characteristic impedance of 50 Ω. What is the magnitude of the incident voltage $\hat{V}_{FWD}$ and of the return voltage $\hat{V}_{BACK}$?

Solution:

Since the generator, at first, does not "know" yet the terminating resistor at the end of the cable, the

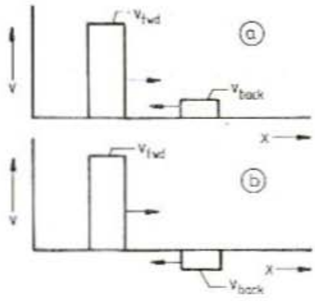

Fig. 3: Partial reflection
a) tending to open-circuit
b) tending to short-circuit
Magnitude of reflection factor
$r = \hat{V}_{BACK} / \hat{V}_{FWD}$

incident pulse amplitude is determined by the proportional impedance existing between the generator and the cable. The generator "sees" the cable impedance (but not the load impedance).

Since $R = Z_o$ then the voltage splits equally across these impedances (i. e. $\hat{V}_{FWD} = \hat{V}_o / 2 = 10$ V). A current pulse $\hat{I}_{FWD}$ is also associated with the incident wave which has an amplitude $\hat{V}_{FWD} / Z_o = 10\ V / 50\ \Omega = 0.2$ A. Owing to the mismatch at the cable-end, the forward pulse is partially reflected and a voltage $\hat{V}_{BACK}$ is formed together with a current $\hat{I}_{BACK} = \hat{V}_{BACK} / Z_o$. What their magnitude and sign is, depends upon the mismatch. For this particular case, tending towards open-circuit termination ($R_L > Z_o$), the forward and return pulses have the same polarity voltage and they add $\hat{V}_{FWD} + \hat{V}_{BACK}$ across the load resistor. The forward and return currents, however, have opposite polarities (high R_L therefore small load current) and the total composite current through the load is:

$$I_L = \hat{V}_{BACK} (\hat{V}_{FWD} / Z_o - \hat{V}_{BACK} / Z_o)$$

The resultant $\hat{I}_{BACK}$ forms so that ohm's law is fulfilled at the load.

$$\hat{I}_{BACK} = \hat{V}_{FWD} + \hat{V}_{BACK} = (\hat{V}_{FWD} / Z_o - \hat{V}_{BACK} / Z_o) R_L$$

I. e. the total voltage at the cable end = the total current times the load resistance.

After putting in figures, a simple equation remains, which will give the unknown, namely $\hat{V}_{BACK}$

$$(10\ V + \hat{V}_{BACK}) = (10\ V / 50\ \Omega - \hat{V}_{BACK} / 50\ \Omega) : 75\ \Omega$$

re-arranging:

$$\hat{V}_{BACK} = 10\ V\ (75\Omega - 50\Omega) / (75\ \Omega + 50\ \Omega) = 2\ V$$

2.3. Reflection Coefficient

The fraction in the above example gives the factor which, when multiplied by the incident voltage, results in the amplitude of the return voltage. This factor is known as the reflection coefficient r. In general, the formula in terms of an ohmic load:

Reflection coefficient $r = (R_L - Z_o) / (R_L + Z_o)$.

Referring to fig. 2 c $R_L = Z_o$ and therefore the reflection coefficient r = 0. (no reflection). In fig. 2 b, $R_L = \infty$ therefore r = 1 (total reflection). The situation depicted in fig. 2 a results also in total reflection but $R_L = 0$, therefore $r = -1$. The sign change indicates that although forward and return voltages posses equal amplitudes, i. e. total reflection, the polarity of the return pulse is negative compared with that of the incident pulse. (see also fig. 1 a).

Fig. 3 shows the case of partial reflection, **fig. 3 a** shows that tending to infinate resistance, and **fig. 3 b** shows that tending to zero resistance.

Example:
In fig. 3, $\hat{V}_{FWD} = 2.5$ V. The 50 Ω cable is terminated with 75 Ω. What is the amplitude of the reflected pulse?

Solution:

$$r = (75\ \Omega - 50\ \Omega) / (75\ \Omega + 50\ \Omega) = 0.2.$$

therefore,

$$\hat{V}_{BACK} = 2.5\ V \times 0.2 = 0.5\ V.$$

Note:
When the line losses are finite, quite large errors can be introduced by the cable attenuation. The return pulse arriving back at the generator has been attenuated twice, once on the incident journey and then on the return journey.

Example:
The complete cable has an attenuation of 1.5 dB. The forward has an amplitude of 2.5 V. The cable

has a characteristic impedance of 50 Ω and is terminated with a load resistor of 75 Ω. With what amplitude does the reflected pulse arrive back at the generator?

Solution:
The incident pulse appears at the cable end attenuated by

$$1.5\ \text{dB i. e.} \triangleq 1.19,$$
$$\hat{V}_{FWD\,(term.)} = 2.5\ V / 1.19 = 2.1\ V$$

as a consequence of the mismatch

$$r = (75\ \Omega - 50\ \Omega) / (75\ \Omega + 50\ \Omega) = 0.2$$

and the magnitude of the return voltage is:

$$\hat{V}_{BACK\,(term.)} = 2.1\ V \times 0.2 = 0.42\ V$$

Upon the return journey this voltage experiences a further attenuation of 1.5 dB

$$\hat{V}_{BACK\,(gen.)} = 0.42\ V / 1.19 = 0.35\ V$$

This means that, because of the attenuation the reflection coefficient r = 0.35 V / 2.5 V = 0.14 i. e. 14 % instead of 20 % neglecting attenuation.

3. MEASURING WITH PULSES

From the reciprocal of $c = 300 \times 10^6$ m / s (the speed of light through space) the time per metre is obtained. When the velocity through the cable is considered, it is reduced by a factor dependent upon the physical characteristics of the cable. Most coaxial cables have a velocity factor of 0.66 which means that the signal requires some 1.5 ns longer to traverse one metre of cable than it would through one metre of space. Short cables used for pulse measurement require therefore, pulses with rise-times of only a few nano-seconds and an oscilloscope with a bandwidth of a few tens of MHz. In order to reduce the requirements upon the test equipment, it is better to use a longer cable of length say, from 50 to 100 m. By this practice, the pulses may be clearly displayed using a generator with a rise-time of 0.1 to 0.5 µs and an oscilloscope of only a few MHz bandwidth.

Konrad Hupfer, DJ 1 EE

SSB Mini Transverter 144 / 1296 MHz

The following article describes a small transverter for the 2 metre to 23 cm band which should awaken the interest in SHF home construction and with it, the activity on this interesting band.

1. CONCEPT

In order that the transverter **(fig. 1)** may be simpler to reproduce, the construction is carried out as far as possible using the printed circuit board (PCB) technique. The epoxy-glass PCB is housed in a tin-plate box of external dimensions (148 x 74 x 30 mm). The well-known 2 metre transceiver IC 202 is used as the basic equipment for transmit drive and receive functions. The IC 202 transmit power of 3 W is reduced, by a simple means, to about 10 mW which is then translated by the transverter to the 23 cm band at a power of 500 mW. This sort of power is relatively easy on batteries and the small total weight makes it ideal for use in mobile and / or field days.

The Tx / Rx switching in accomplished by means of a 3.5 V (approx.) control voltage which is taken

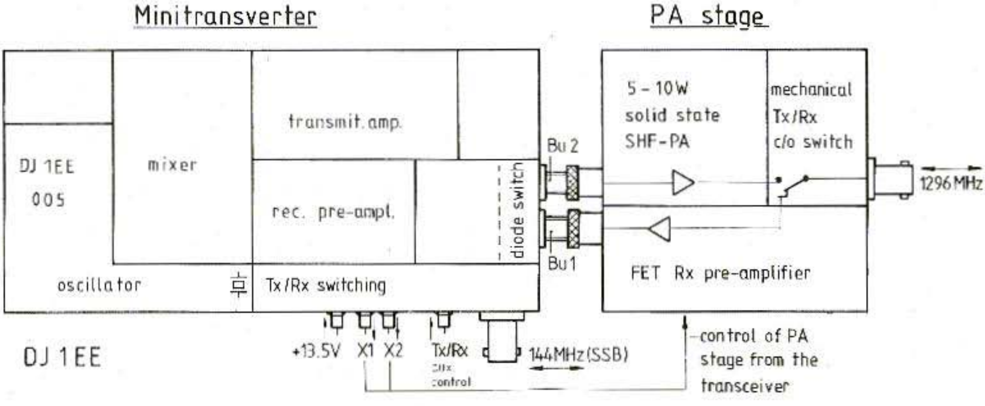

Fig. 1: Main constructional layout of 144 / 1296 MHz mini-transverter and its companion PA / Rx preamplifier (to be described later)

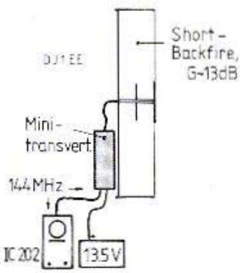

Fig. 2:
Portable operation of transverter

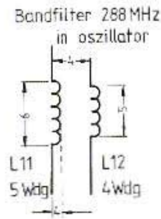

Fig. 4:
288 MHz L. O. band-pass filter

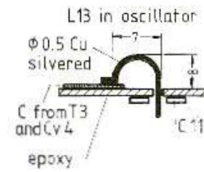

Fig. 5:
Construction of L 13 in L. O.

from the IC 202 on "receive" via its antenna socket. The only connection between the transverter and the 2 metre equipment, IC 202, is a 50Ω coaxial cable for the 2 m signals and the Tx / Rx switching. The 13.5 V transceiver power is derived from a separate battery supply. The small and light-weight transceiver itself, can be mounted directly at the antenna terminals in order to avoid cable losses. The author mounted his transverter behind the reflector of a Short-Backfire-antenna with a gain of 13.5 dB_d for portable operation **(fig. 2)**.

The mini transverter can also be employed for fixed-station use by the addition of a 5 W amplifier and low-noise preamplifier which will be described in a later article. The necessary supplies and control for this appendage being taken via the transverter.

Just because this transverter is offered in kit-form with all the required parts, it does not have to result in a slavish copying of the authors prototype. Parts which are on hand should be tried and perhaps other transistors should be experimented with. The first two examples built on the final PCB did show a few minor differences caused by component tolerances.

2. CIRCUIT DESCRIPTION

The complete circuit schematic of the mini transverter is shown in **fig. 3.**

2.1. Oscillator

The crystal oscillator runs at 96,000 MHz from a stabilised supply. It uses transistors BFR 90 / BFR 91 / BFR 91 A and the output circuit L 1 / C 1 is tuned to 96 MHz. Transistor T 2 (BFR 90 / 91 A) is coupled via C 5 and functions as a tripler. The resulting frequency of 288 MHz at L 11 / Cv 2) is taken via a bandfilter (L 12 / Cv 3) to the base of transistor T 3 which functions as a doubler. The matching from T 3 to T 2 is optimised by means of the coupling (**fig. 4**) from L 11 / L 12 in order that T 3 passed a maximum current. The signal at **L** 13 / Cv 4 (**fig. 5**) is at 576 MHz and is passed to a further doubler stage T 4. The inductance of the output filter is formed by the PCB and at its output is a power of 40 mW (BFR 34) at 1152 MHz. The bandfilter is tuned for a maximum in the mixer diodes at test point M 1/2.

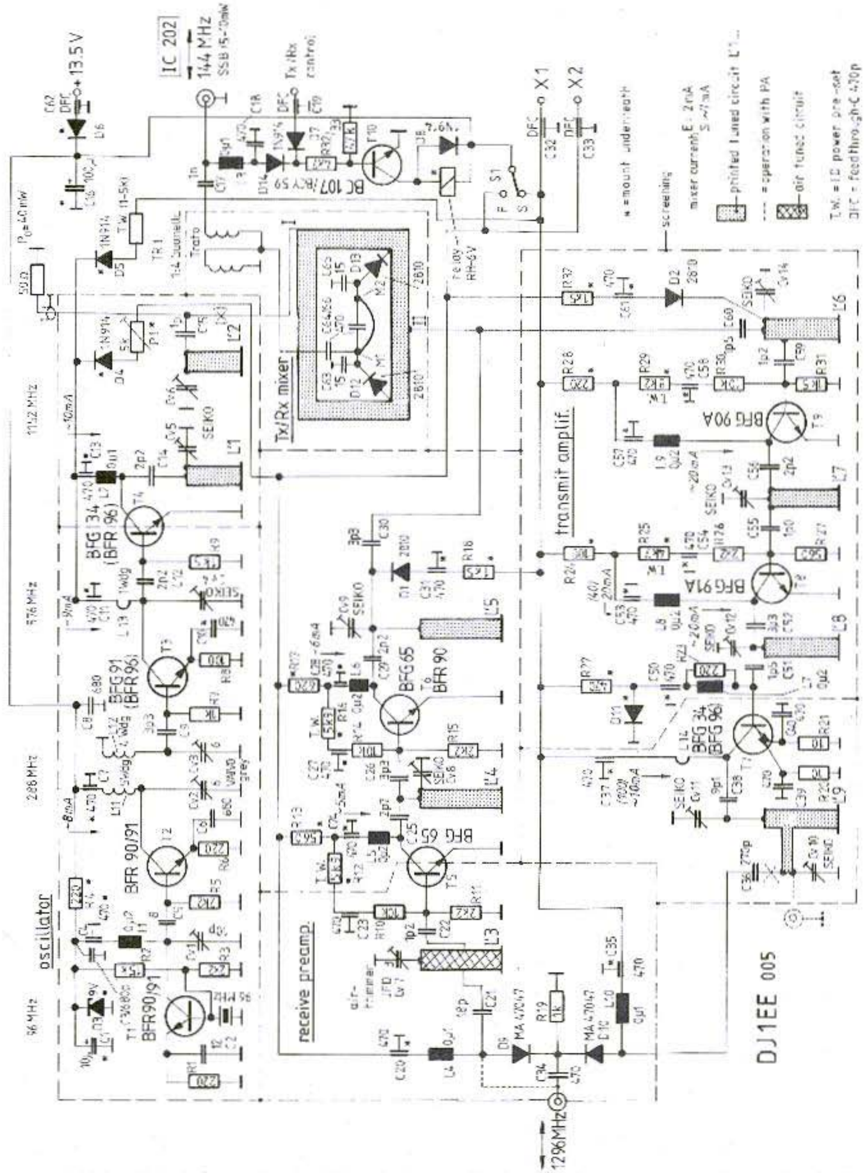

Fig. 3: Complete transverter circuit schematic

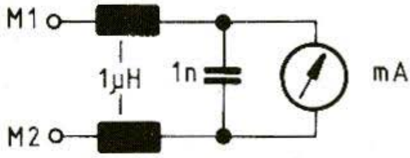

Fig. 6: Test meter for alignment purposes

In the "transmit" mode the maximal oscillator power of 40 - 50 mW is produced; the power supply for T 3 and T 4 is taken via diode D 5 and a selected resistor. This resistor is selected for a mixer current of approx. 10 mA on "transmit" directly from the battery potential rail.

On "receive", T 3 and T 4 are fed a reduced voltage via P 1 and D 4. The potentiometer P 1 is so adjusted that a 2 mA mixer current flows between testpoints M 1 and M 2.

2.2. Transmit / receive mixer

The same ready-to-hand 180° ringmixer was used both for transmit and receive.

The bridge is removed from points M 1 and M 2 and replaced with the meter test circuit of **fig. 6**. The same procedure as in 2.1. is used for the requisite mixer currents.

On "transmit" a signal (approx. 10 mW) at 144 MHz is fed from the IC 202 via a 4 : 1 transformer and C 64 to the diodes D 12 and D 13. At the mixer output II the both sidebands f_1 = 1152 MHz + 144 MHz and f_2 = 1152 − 144 MHz are present. The oscillator frequency is suppressed by some 18 dB. The wanted frequency, f_1 = 1296 MHz, is selected by the parallel circuits in the three-stage transmit amplifier. In order that no transmitted signal appears in the receiver preamplifier, the circuit Cv 9 / L 5 is strongly detuned by diode D 1.

On "receive" mode, point II of the mixer is fed by the amplified (20 dB approx. by T 5 and T 6) input signal. The IF signal of 144 MHz, developed in the mixer, is taken via C 64 and TR 1 to the SSB transceiver. In order that the transmit tuned-circuit L 6 / Cv 14 does not load the receive signal it is detuned by diode D 2.

2.3. Transmit amplifier

The selected sideband at mixer output II is fed at a level of 1 mW into a three-stage linear amplifier by which it is amplified to a power of at least 500 mW (27 dBm). The newly introduced Valvo plastic transistors BFG 90 A / 91 A / 96, intended for the 900 MHz mobile-telephone application, are used in this amplifier. They are eminently suitable for use at 1296 MHz and, with their two emitter connections, represent a considerable inprovement on the BFR 90 / 96 series.

The circuit is quite staight-forward; as already mentioned, three tuned RF amplifiers are in tandem. The preset R 29 adjusts the quiescent current through T 9 to 20 mA. A power of 10 mW (approx.) is available at L 7 / Cv 13. In order to measure this, C 55 is removed from the base of T 8 and 50Ω cable connected to it – the cable screen should be connected as directly as possible to ground. –

The preset R 25 sets the quiescent current for T 8 at 25 mA. This stage delivers approx. 120 mW / 50Ω on signal peaks and at a peak collector current of some 40 mA. The same method is used to measure the output power, C 51 being used for the coupling to the test cable.

The quiescent current of T 9 is set to 10 mA, this being adequate for linear operation. On signal peaks the collector current is driven to 110 mA approx. This stage can employ the BFG 34 if a power output of 1000 mW is required but the BFG 96 will supply some 500 mW to the output. The BFG 34 is to be preferred, however, owing to its higher power dissipation capabilities. At ambient temperatures in excess of 55° C, prolonged continuous wave outputs should be strictly avoided.

The output power developed at C 38 / Cv 11 / L 9 / Cv 10 is routed in the "transmit" condition via

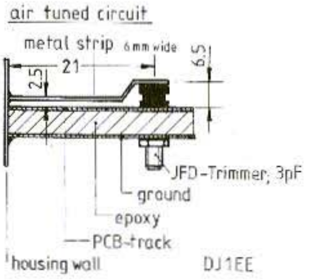

Fig. 7: Low-loss version of Rx input circuit

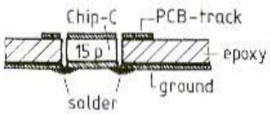

Fig. 8: Proposal for using chip capacitors at microwaves

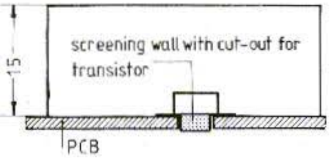

Fig. 9: Mounting the screening walls over a transistor

PIN-diode D 10 to the output socket of the equipment. When operating with the output stage mentioned earlier, the output line is interrupted after C 36 and the 1296 MHz transmit signal is taken to a specially provided BNC panel socket for the supplementary output amplifier.

2.4. Receive preamplifier

Under "receive" conditions, the PIN-diode D 9 conducts and the signal from the antenna is led via a parallel-tuned circuit to the first low-noise transistor amplifier stage using a BFG 65. In order to avoid the sort of losses inevitable in PCB tuned circuits, the Q is raised considerably by constructing the input tuned circuit from a high-quality feed-through microwave trimmer capacitor and a metal strip inductor supported in air as shown in **fig. 7**. The preamplifier is capable of a 20 dB amplification at a noise-figure of about 2 dB inclusive of diode switch. The mixer conversion loss is about 10 dB, therefore, in the interests of simplicity, an additional IF amplifier was not thought necessary. By means of the preset resistors R 12 and R 16 the appropriate transistor currents are set at 5 and 6 mA respectively. L 3 / Cv 7 input tuned-circuit is adjusted initially for maximum IF output and then for maximum signal noise ratio.

2.5. Transmit / receive switching

On the IC 202 transceiver "receive" position, the control circuit voltage switches the Tx / Rx relay RS 1 via transistor T 10. The supplies are thereby switched to the individual circuits used for reception. An auxiliary voltage output, isolated by D 7, is available for controlling other equipment, for example, the inclusion of the mini transverter into fixed-station use together with the projected supplementary output amplifier / receive preamplifier.

3. CONSTRUCTION

The PCB, DJ1EE 005 is loaded with the components in accordance with the location plan of **fig. 15** and the photographs of **fig.s 16 and 17**. Particular construction points are high-lighted in **figs. 7 to 14**. A few points concerning the high-frequency construction and special tuning instructions will now be given.

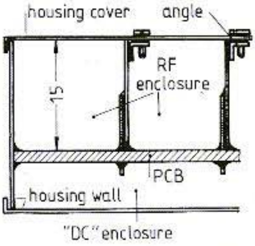

Fig. 10: Vertical cross-section through transverter

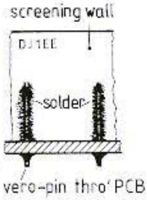

Fig. 11: Grounding and fixing of screening walls

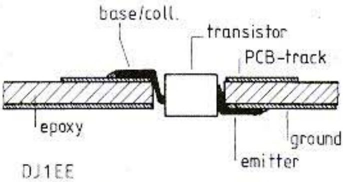

Fig. 12: Installing the microwave transistors

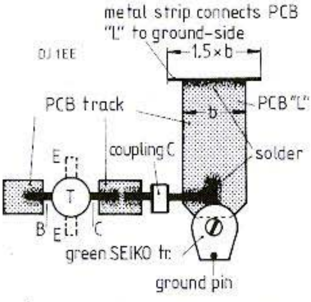

Fig. 13: Further details of microwave construction

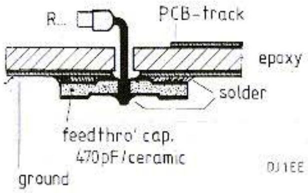

Fig. 14: Installing feed-through disc capacitors

All Seiko-trimmers are installed in such a manner that the stator is fitted through a hole in the PCB and soldered to the copper surface. The rotor connection (thin tab) is bent to make contact with the hot end of L 13 or striplines L 1 to L 9 according to **fig. 13**. This unusual manner of construction, with the rotor being the "hot" component of the capacitor, requires the use of a non-metal trimming-tool but has the advantage of a rigid connection to the appropriate inductance. The screening walls should be soldered to supporting veropins which have been inserted in the PCB at 10 mm intervals and which have been soldered to the copper surfaces of the PCB. (**see figs. 10 and 11**). **Figures 9, 12 and 13** should be studied before installing the transistors.

The ceramic coupling capacitors between stages are soldered with connection leads being as short as possible, see **fig. 13**.

The cold ends of the stripline tuned circuits are also secured with a tin-plate metal tab which is fed through a slot cut in the PCB, and soldered to the back surface of the board.

3.1. Components

Cv 1: Foil trimmer 10 pF (Valvo : yellow)
Cv 2, Cv 6: Mini foil trimmers 3 pF (Seiko : green)
Cv 7: Microwave air trimmer (Johanson, Tekelec)
Cv 8, Cv 14: Mini foil trimmers 3 pF (Seiko : green)
C 5, C 9, C 11 etc.: Ceramic coupling capacitors (soldered with short leads)
C 39, C 40, C 63, C 65: Ceramic chip capacitors (Valvo, ATC)
Inductance: see sketches
TR 1: Guanella-trnsfr. 1 : 4 with twin-hole core, Siemens: Material U 17, ht. 8.3 mm or 6.2 mm, twisted CuL wire 0.2 mm dia, 45 mm long and connect as 1 : 4 transformer. The 2.5 mm core is also used if 0.1 mm wire is employed.
D 1, D 2, D 12, D 13: Hot-carrier-diodes HP 2810
D 9, D 10: PIN-diodes MA 47047
D 11: 1 N 4001 or similar
All other diodes: 1N 914, 1N 4148 or similar
T 1, T 2: BFR 90, BF 91

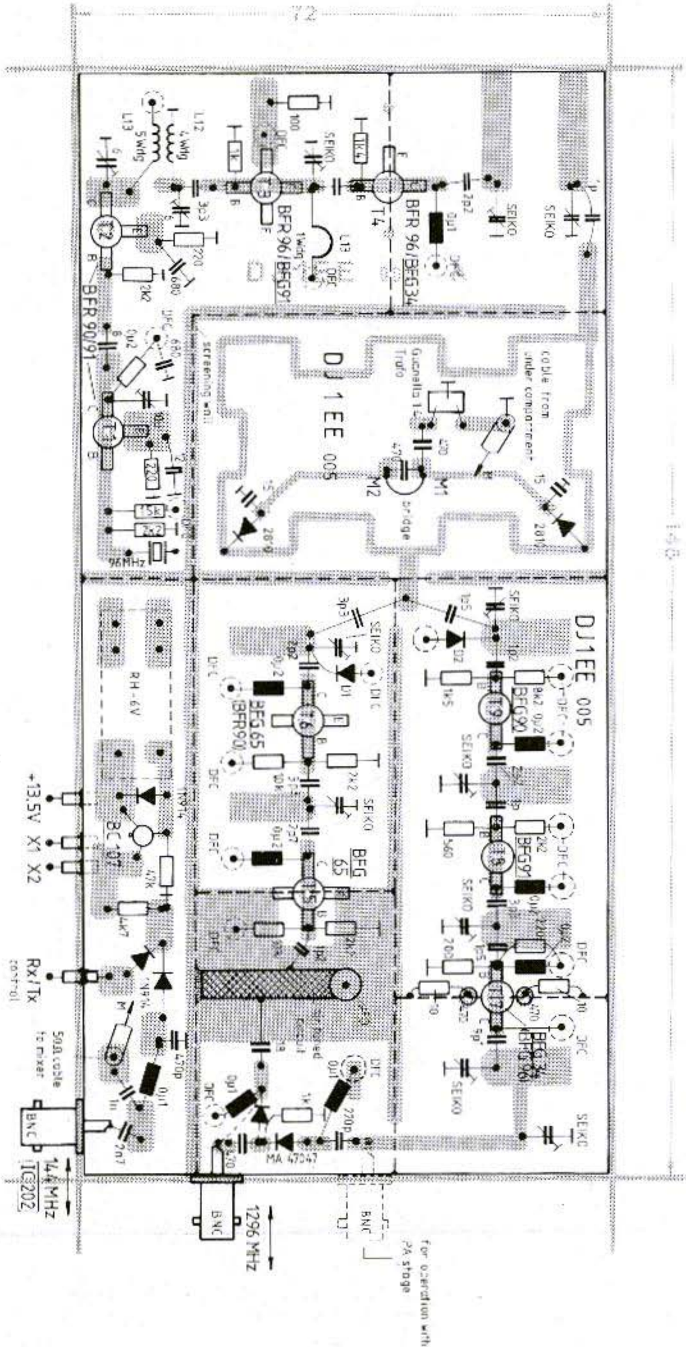

Fig. 15:
Printed circuit board DJ1EE 005 showing components mounted on track-side

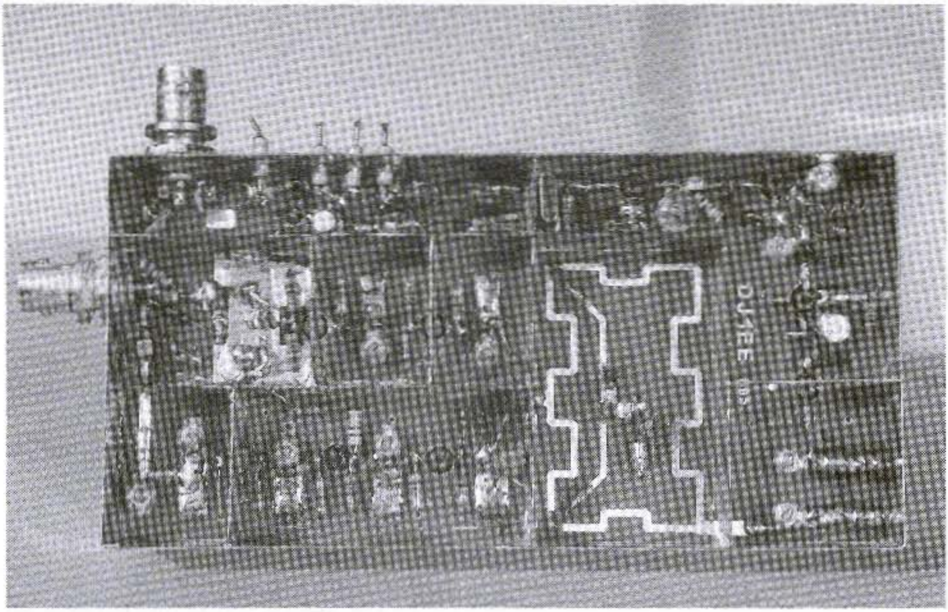

Fig. 16: Component side of "rough" test construction

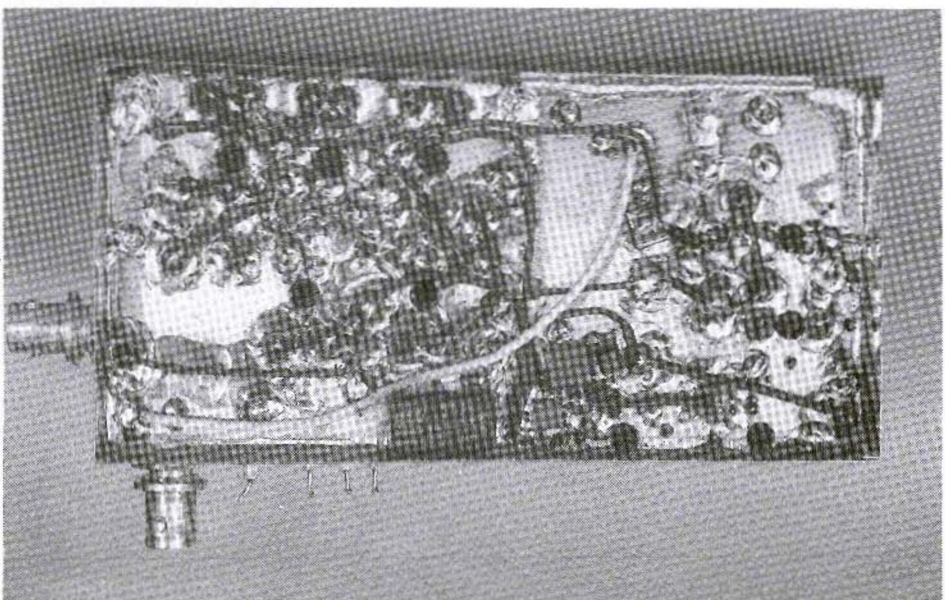

Fig. 17: Underneath view of prototype

T 3: BFG 91A (BFR 96)
T 4: BFR 34
T 5, T 6: BFG 65
T 7: BFG 34 (BFG 96)
T 8: BFG 91A (BFG 90A)
T 9: BFG 90A (BFG 91A)
R 22: 0.5 W type (0309)
all other resistors: smallest type (0207 or smaller)
Instead of the 9 V zener D 3 with resistor R 4, a 9 V IC regulator can be used.

Post up

On the circuit diagram and component layout plans there are several alternative transistors indicated for the oscillator and the receive preamplifier. This means that the well-known BFR 90 / 96 can also be used, but small alterations in the size of the coupling capacitors must be made. The transmit amplifiers, however, should retain the higher gain BFG 90 A / 91 A types.

Joachim Kestler, DK 1 OF

Two-Metre Receiver Front-End

The following has not been written merely to swell the ranks of two-metre front-end articles which have become prevelent in recent times. Rather, it is an attempt to present a module, which possesses respectable specifications and is capable of alignment by the amateur without access to professional test equipment.

The complete circuit has been divided into two modules (1), the pre-amplifier (2), the mixer complete with oscillator and driver. This two-part construction offers increased flexibility when combining the front-end with other equipment e.g. UHF / SHF converters. Also, the pre-amplifier may be separated from the main equipment and mounted directly behind the antenna in order not to de-

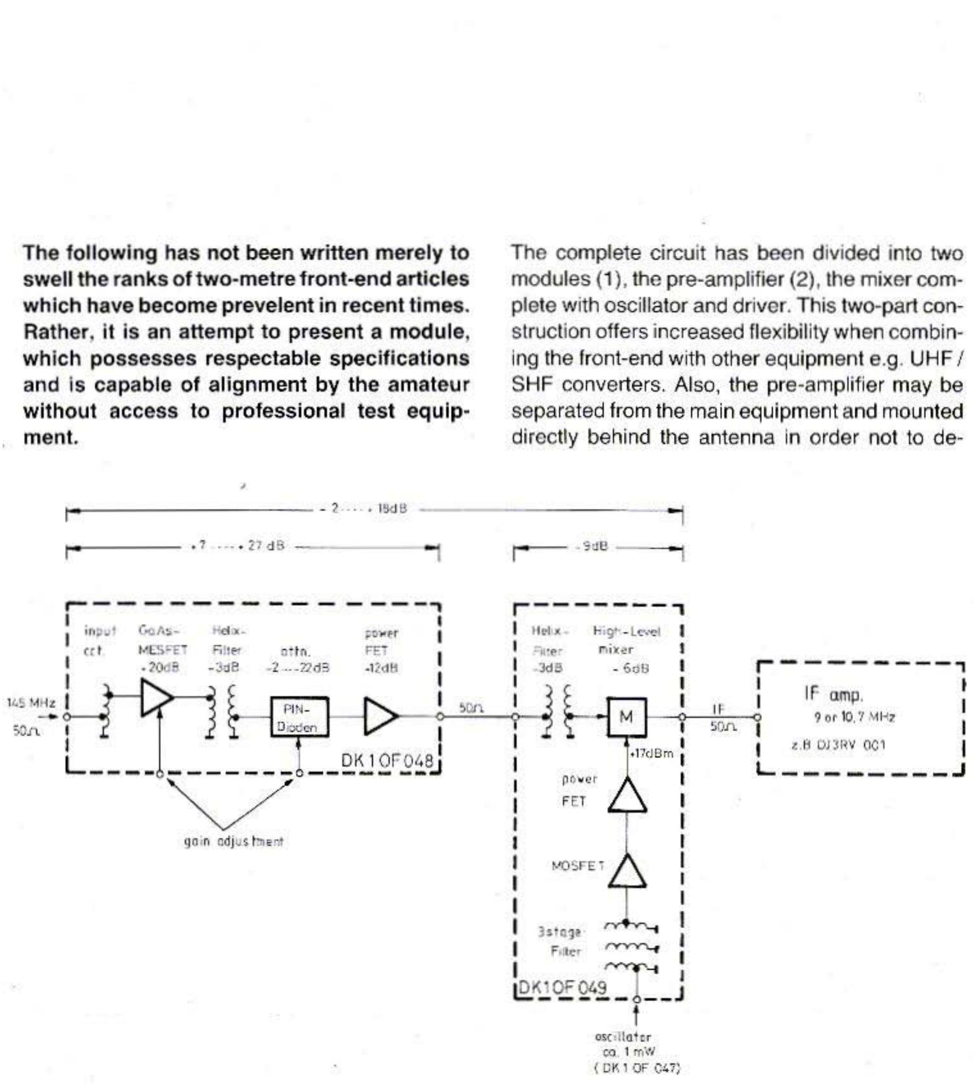

Fig. 1: 2 m-Front-end block diagram indicating stage levels

grade the overall noise-figure by a long cable run. The mixer portion however, has been specially designed for use with the PLL delay-line oscillator described in (1) but may be used, of course, with any oscillator of appropriate frequency and 1 mW/50Ω output.

1. CONCEPT

The block diagram of the front-end is shown in **fig. 1**. A self-supporting coil serves as part of the input tuned circuit and impedance match from antenna cable (50Ω) to the pre-amplifier input transistor (about 800Ω). The latter is fitted with a GaAs-MESFET enabling a noise-figure of 1 dB (approx.) to be achieved. Following a two-circuit helix-filter is a variable PIN-diode attenuator. This attenuates signals to the next pre-amplifier stage and mixer according to the prevailing input conditions, thus enabling high gain for weak incomming signals but preventing receiver overloading during strong signal reception. The second amplifying stage is a high-current, barrier FET whose output is delivered to the next module, the mixer, via a 50Ω coaxial cable.

It could be asked, at this stage, why not use the pre-amplifier concept suggested by DJ 7 VY in (2) using push-pull transistors. Certainly, the published data speaks for itself and it is able to be reproduced with the full specifications, at least, when terminated by broadband real 50Ω impedances on input and output. Using high Q helix-filters with this circuit however, the author found that spurious oscillations above about 1 GHz, were not easily discouraged without compromising the

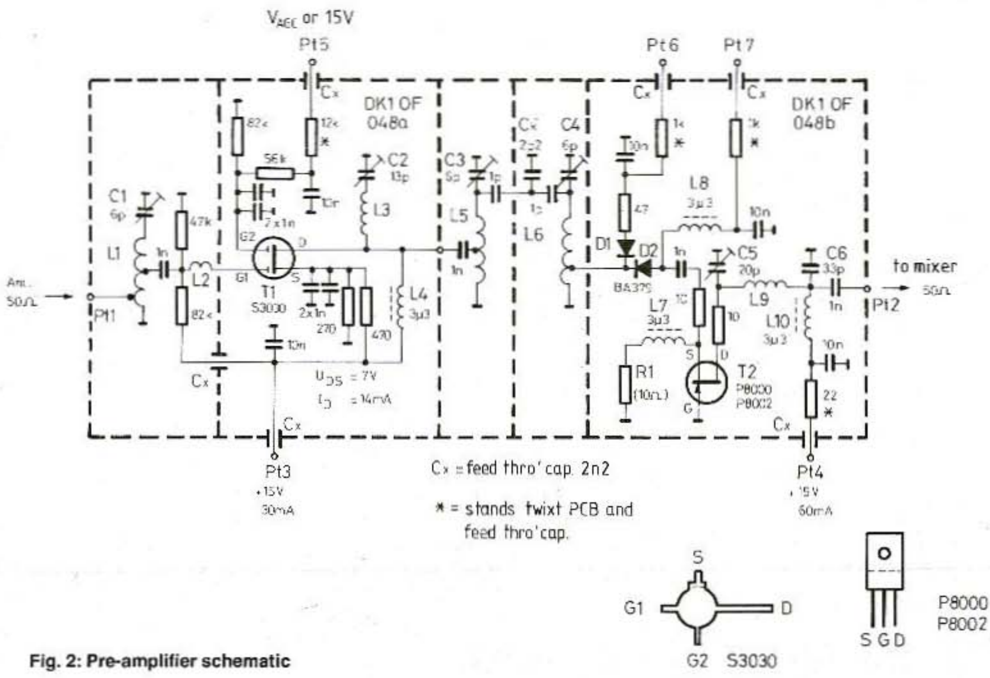

Fig. 2: Pre-amplifier schematic

specifications. It was decided therefore, to dispense with the "super I.P. specification concept" in the interest of reasonable performance with sure-fire reproduction capabilities.

A high-level hot carrier diode ring-mixer follows the two-stage helical filter. The necessary oscillator power 17 dBm (= 5o mW) is supplied by a two-stage amplifier comprising a MOSFET first stage and a high-current FET second stage which drives the mixer L. O. port across a 50 Ω terminating impedance. A three-circuit input bandpass filter is provided for the L. O. amplifier in order that the incoming local-oscillator multiplication signals (fo / 2, 3 fo / 2 etc.) contained in the output of module DK 1 OF 047, are suppressed. The mixer IF port, should be terminated with an IF amplifier first stage, possessing a wide-band 50 Ω resistive input impedance together with a noise figure of 6 dB or lower. The necessity for a ring-mixer IF port to be so terminated has been dealt with at large and in references (3) and (4).

2. CIRCUIT DETAILS

2.1. Pre-amplifier

The detailed circuit schematic of the pre-amplifier is shown in **fig. 2**. The GaAs-FET first stage is preceded by an input filter L 1 / C 1. The drain-current is 14 mA, a compromise between lowest noise figure (8 mA) and high intercept capabilities. The transistor source and gate 2 electrodes are double decoupled to reduce the deleterious effects of electrode lead inductance. The choke L 2 (ferrite bead) at gate 1 is not absolutely necessary, as in the prototype at least, no spurious oscillations broke out when it was removed. The "suck-out" circuit L 3 / C 2 is tuned to the image-frequency (approx. 125 MHz) and presents a low impedance at this frequency. The connection pt. 5 is intended for an automatic gain control but this can only be recommended in cases of poor AGC action in the IF amplifier. The application of AGC to pt. 5 will compromise the large signal handling capabilities of the GaAs-FET and it is better to supply it with a fixed + 15 V instead.

The following two-stage helical filter (L 5 / C 3 and L 6 / C 4) is slightly over-coupled (midband dip approx. 1.5 dB) in order to achieve the necessary 2 MHz bandpass. For pure SSB / CW use, C_K may be increased to some 6 - 8 pF thereby reducing the coupling and the bandpass to some 600 kHz.

For gain adjustment purposes, the PIN-diode D 2 is utilised which is supplied by the signal-controlled direct current via pt. 7. In order that the helical filter is properly terminated under all signal conditions, thus preserving its bandpass, the PIN-diode D 1 has been provided which passes a complementary bias-current via pt. 6. The second pre-amplifier T 2 with the high current FET, is connected in a grounded gate configuration and in order to secure a high intercept point, a. D. C. input power of almost one Watt must be invested. The amplified input signal is taken via a pi-filter C 5 / L 9 / C 6 to the output pt. 2 where it is connected to the mixer module. **Fig. 3** shows the simple manner by which the PIN-diode attenuator control-current may be provided.

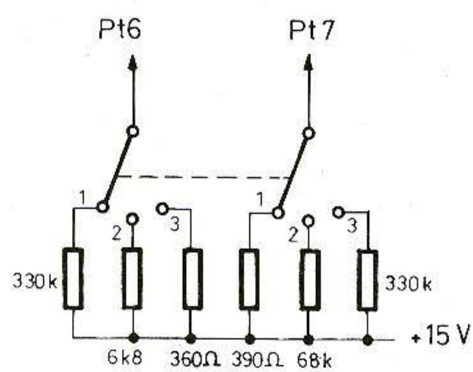

Fig. 3: Biasing the PIN-diode attenuator

switch position	attenuation	overall pre-amp. gain
1	− 2 dB	+ 27 dB
2	− 12 dB	+ 17 dB
3	− 22 dB	+ 7 dB

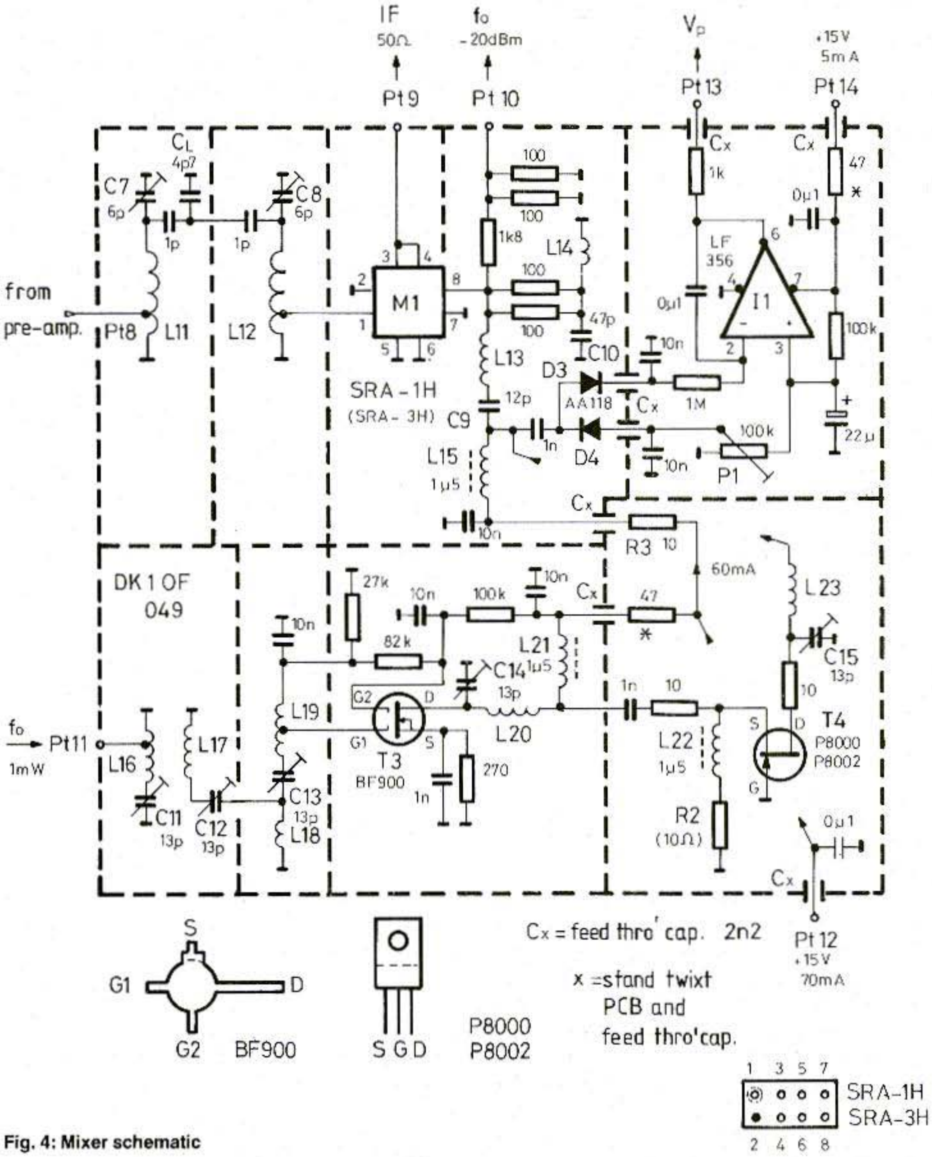

Fig. 4: Mixer schematic

2.2. The Mixer stage

The cicuit schematic of the mixer portion is to be seen in **fig. 4**. The signal delivered by the pre-amplifier is passed via pt. 8 to the second helical-filter (L 11 / C 7 and L 12 / C 8). This is critically coupled, but again, an alteration to the value of the coupling capacitor C_L enables the bandpass to be varied. The ring-mixer which follows, receives the input signal on pin 1 and the generated IF output is taken from pins 3 and 4 to pt. 9 and on to the IF stage. The local-oscillator signal is fed to the module via pt. 11 and to a three-circuit filter L 16 / C 11, L 17 / C 12, L 19 / C 13, L 18 being the coupling element. This filter accepts the local-oscillator signal frequency but rejects harmonics and sub-harmonics. The two-stage oscillator consists of transistors T 3 (driver) and T 4 (power amplifier). These transistors operate in class A requiring a higher current consumption than class B or C, but having the advantage of giving a clean, noise-free translating signal. The L. O. signal is then fed into a duplexer C 9 - L 13 - C 10 - L 14 and from that into the mixer pin 8. The necessity for the duplexer is discussed in detail in reference (4). A portion of the L. O. signal (− 20 dBm approx.) is tapped-off before being applied to the mixer and taken to pt. 10 for possible use in a frequency counter or the transmitter mixer. The diodes D 3, D 4 produce a DC voltage which is proportional to the L. O. signal and is taken via an operational amplifier IC 1 and pt. 13 to pt. 4 of the oscillator DK 1 OF 047 module as a control voltage. In this manner the mixer input power can be made to remain constant despite variations due to ageing and temperature. The L. O. input power is controlled by P 1. The control amplifier IC 1 is supplied with 15 V DC via pt. 14 whilst the DC supply for the module is introduced at pt. 12.

3. CONSTRUCTION

For both circuits, double-sided, through-contact PCBs have been designed. The use of tin-plate for screening the VHF high Q circuits is not recommended (1), therefore there was no need to dimension these PCBs in order that they would fit a proprietary shielded box. Instead, a strip of 0.5 mm sheet brass some 30 mm wide is soldered around the edges of the PCBs in order to form a frame, the PCB conductor side sitting some 8 mm up from the lower edge of the brass frame.

Figs. 5 and 6 show the dimensions and the major part locations for both modules, and **figs. 7 and 8**

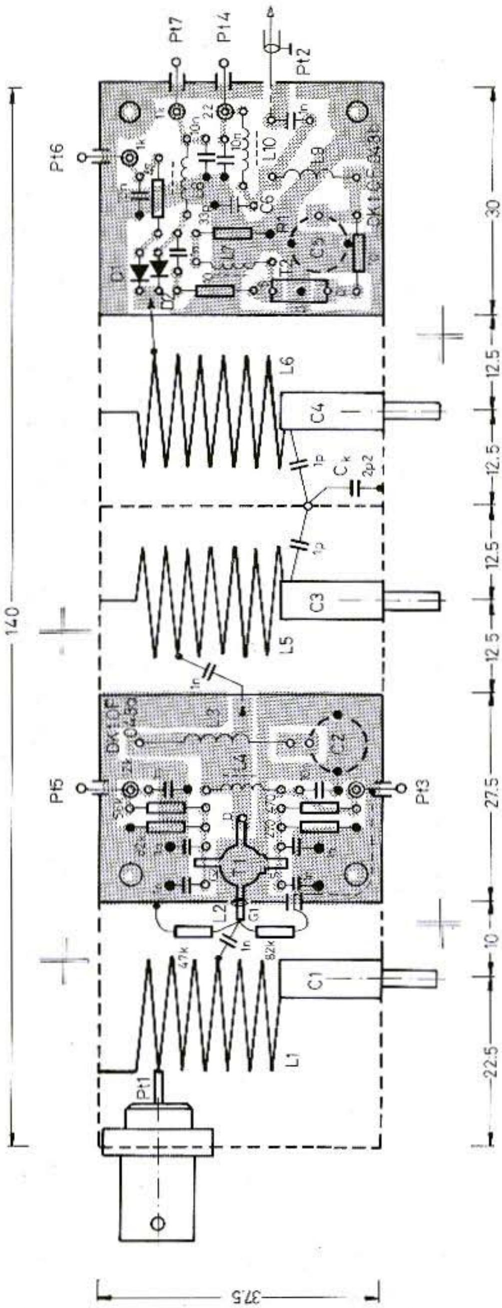

Fig. 5: Construction and main component layout of pre-amplifier DK 1 OF 048

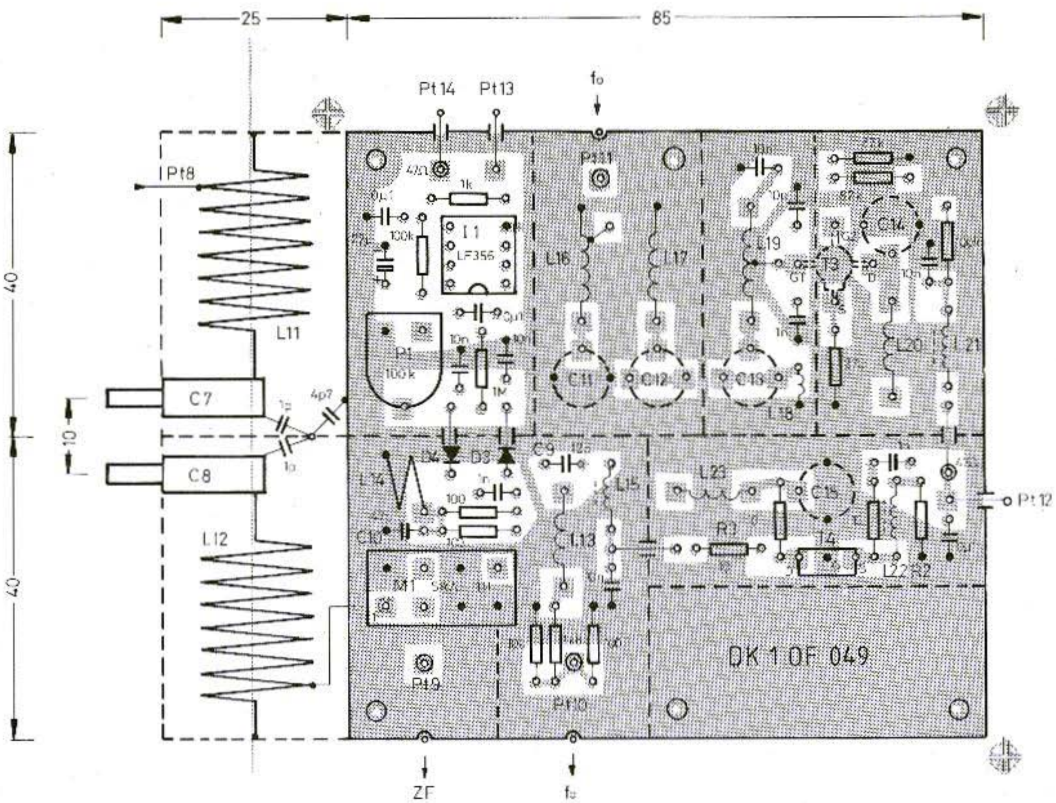

Fig. 6: Construction and main component layout of mixer DK 1 OF 049

are photographs of the prototypes. Now for one or two of the finer points of detail: The gate 1 connections of both T 1 and T 3 are fed straight through holes drilled in the screening wall, just **above** the PCB surface, the transistors being totally surface-mounted and soldered on the component side of their respective boards. The taps on the helical coils L 5, L 6 and L 12 should be as short as possible and should pass through the screening walls on the underside (track-side) of the PCB albeit, just **below** its surface. The inter-module connection pt. 2 to pt. 8 is effected by means of thin 50Ω coaxial cable (RG 174) directly soldered, or mini– BNC or SMC connectors may be employed. The length of the interconnecting cable is not critical – within reason. The GaAs-FET T 1 is the **very last** component to be soldered-in in order to minimise the risk from static damage during the construction. The P 8002 transistors have unusually long cooling tabs which would protrude above the level of the screening walls. They should be shortened by 5 mm, bent at right angles and soldered to the screening wall thus increasing the heat sinking efficiency. The soldering, however, should be carried out as quickly as possible and with an adequately rated, hot solderin-iron.

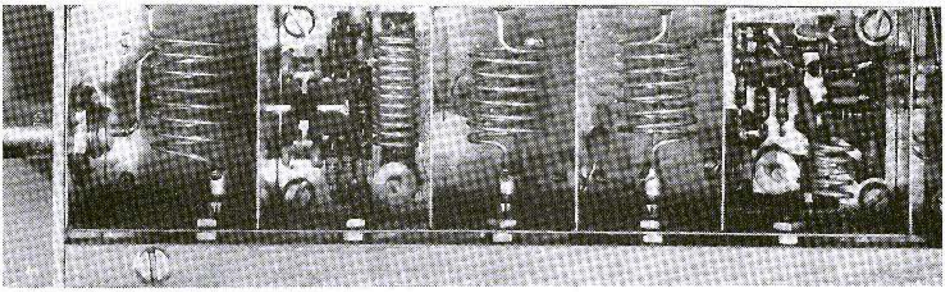

Fig. 7: Pre-amplifier module DK 1 OF 048

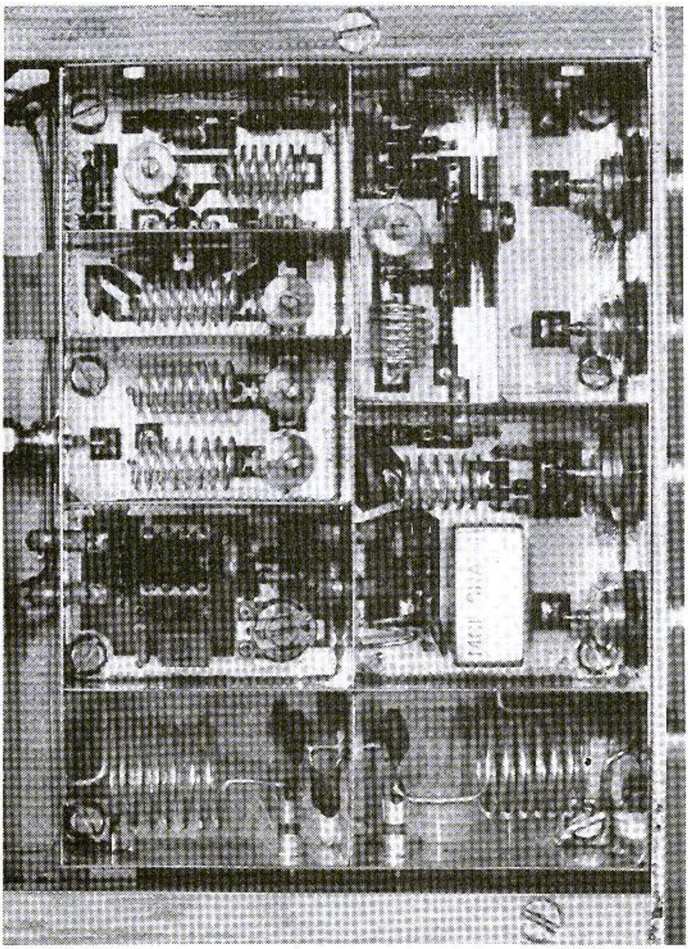

Fig. 8:
Mixer module
DK 1 OF 049

4. SPECIAL COMPONENTS

T 1:	GaAs-MESFET S 3030 or S 3000 (older type) (Texas Instruments)
T 2, T 4:	P 8000 or P 8002 (T.I.)
T 3:	BF 900 (T.I.) or BF 961, BF 963 (Siemens)
IC 1:	LF 356 N (DIP) or LF 356 H (TO - 99), various manufacturers
D 1, D 2:	PIN-diodes BA 379 (Siemens)
D 3, D 4:	AA 118 or similar Ge-diodes
M 1:	Hot-carrier-diode ringmixer SRA-1H or SRA-3H or TAK-1WH (Mini-circuits)
C 1, C 3, C 4, C 7, C 8:	Ceramic tube trimmer 3 mm dia, 6 pF
C 2, 11, 12, 13, 14, 15:	Foil-trimmers, 7.5 mm dia, 13 pF (yellow)
C 5:	Foil-trimmer, 7.5 mm dia, 20 pF (green)
Electrolytic 22 μF:	16 VDC, 5 mm lead spacing

All other capacitors ceramic disc or multilayer type

P 1:	Preset potimeter 100 KΩ horiz. leads 10 / 5 mm

5. COIL DATA

L 1:	7.5 turns, 1 mm Cu silvered, 13 mm int. dia, 20 mm long tapped for pt. 1 one turn from cold end, tapped for FET 4.5 turns from cold end.
L 2:	Ferrite bead or twin-holed core (Siemens B 62152 - A 8 - X 17) slipped over T 1's gate lead (as required).
L 3:	12 turns 1 mm Cu silvered, 6 mm int. dia, 20 mm long
L 5:	7 turns 1 mm Cu silvered, 13 mm int. dia, 15 mm long, tapped 1.5 turns from cold end.
L 6:	as L 5, but tapped 0.5 turn from cold end.
L 9:	5 turns, 1 mm Cu silvered, 6 mm int. dia, 11 mm long.
L 11, L 12:	as L 5, but tapped 0.75 turns from cold end.
L 13:	6 turns, 1 mm Cu silvered, 6 mm int. dia, 12.5 mm long.
L 14:	1.5 turns, 1 mm Cu silvered, 6 mm int. dia, 5 mm long.
L 16:	8 turns, 1 mm Cu silvered, 6 mm int. dia, 15 mm long, tapped 0.75 turns from cold end.
L 17:	as L 16, but no tap.
L 18:	0.5 turn, 0.5 mm Cu, 5 mm int. dia.
L 19:	as L 16, but tapped in the middle.
L 20:	7 turns, 1 mm Cu silvered, 6 mm int. dia, 12.5 mm long.
L 23:	6 turns, 1 mm Cu silvered, 6 mm int. dia, 10 mm long.

Chokes:

L 4, L 7, L 8, L 10:	ferrite choke 3.3 μH RM 10 mm (Siemens etc.)
L 15, L 21, L 22:	ferrite choke 1.5 μH RM 10 mm (Siemens etc.)

The winding sense of the coils may be seen from the photographs, the object being to chose the winding sense in order that the tap lead is as short as possible.

6. SETTING-UP AND TUNING

After connecting the supply potential 15 V DC to pt. 3, pt. 4, pt. 5 and pt. 12, the working points of the transistors are checked. This is done on T 1 and T 3 by checking the source potentials to ground. T 1 : V_S = 8 V ± 0.5 V, T 3 : V_S = 2.7 V / + 0.5 V / − 1 V. Large deviations from these tolerances indicate a defective device. The current through T 2 must be measured from pt. 4 and the voltage across R 3 checks T 4. With a suitable choise of source resistors R 1 and R 2 (start with 10 Ω) the drain current is adjusted to 60 mA (tolerance ± 10 mA). If a current of less than 50 mA flows with R_S = 0, then the transistor should be replaced. The PIN-diode control current supply circuit shown in **fig. 3** is connected between pt. 6 and pt. 7 and the pre-amplifier module is connected in front on any available 2 m receiver. C 3, C 4 and C 5 are then tuned for maximum noise (roughly), C 1 is then tuned, to a (weak) 2 m signal applied to the pre-amp. input, for maximum deflection on the "S" meter. A signal generator, which has been tuned to the image frequency (127 MHz for 9 MHz IF and 123.6 MHz for 10.7 MHz IF) is then applied to the input and C 2 is tuned for maximum attenuation. If no signal generator is available, just leave C 2 in its mid position.

The mixer module is aligned by connecting pt. 11 with the output of the local oscillator module and with a 20 kΩ / V voltmeter connected to the D 3 / D 4 (+ Ve to D 3 cathode, − Ve to D 4 anode). The oscillator is tuned to its midband frequency and the supply potential 15 V is connected to pt. 12. C 11, C 12, C 13, C 14 and C 15 are then tuned for maximal output. Some iteration must be employed in tuning to attain a maximum output. This should occur at greater than 4 V. Now the level regulator can be set up by connecting pt. 14 to the supply and pt. 13 to pt. 14 of the oscillator module DK 1 OF 047. Using P 1 the D 3 / D 4 output voltage is adjusted to 2.8 V which occurs at a local oscillator power of 17 dBm (50 mW). This power should not vary when the VFO is tuned across the band. The control voltage at pt. 13 rises to 6 V at the band edges and dips to about 3 V at the midband. Its exact characteristic is influenced by the three stage filter (C 11, C 12, C 13 together with the coupling L 16 to L 17).

After the pre-amplifier and the IF module have been connected to the mixer module, the second helical filter is tuned by C 7 and C 8 for maximum signal level. This concludes the front-end adjustment for the time being anyway. A fine tuning will be undertaken at a later stage when the modules are in position in the completed receiver and with their covers fitted. For the adjustment of a flat characteristic across the band − the helical filter determines this − the spectrum from a frequency calibrator can be used (harmonic-rich 100 kHz calibrator). The adjustment of the input circuit L 1, C 1 is best done with the aid of a weak input signal (sig. gen. or transponder). Tune for best signal to noise ratio.

7. MEASUREMENT DATA

7.1. Noise Figure

Test Equipment: Noise Figure Meter HP 8970 A, with Noise-Source HP 346 A
Pre-amp. alone: F = 0.75 dB (at full gain, switch in **fig. 3** in pos. 1)
Complete front-end:

Switch pos. 1	F = 1.1 dB
Switch pos. 2	F = 2.5 dB
Switch pos. 3	F = 6.5 dB

(all measurements made with mixer looking into an NF of 3.5 dB)

7.2. Gain

Test Equipment: Synthesizer SMS, Vector Analyser ZPV (both R & S)

switch position	pre-amp. alone	complete front-end
1	+ 27 dB	+ 18 dB
2	+ 17 dB	+ 8 dB
3	+ 7 dB	− 2 dB

7.3. Selectivity

Test Equipment: Spectrum-Analyser HP 141 T with plug-in 8554 B (VHF / UHF) and 8552 B (IF)

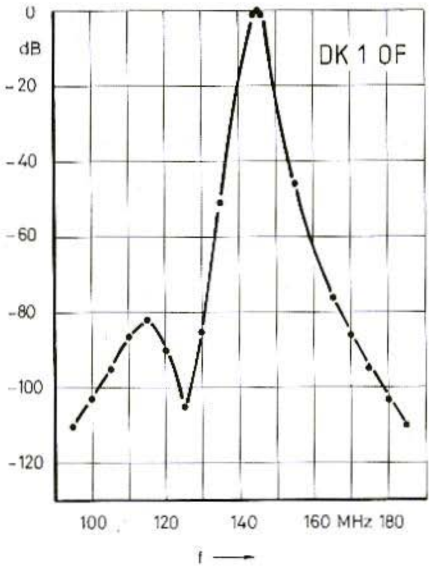

Fig. 9:
Front-end input frequency characteristic

and tracking generator HP 8444 A and SMS + ZPV for values < − 80 dB.

1 dB bandwidth:	2 MHz
3 dB bandwidth:	3.5 MHz
20 dB bandwidth:	10 MHz
60 dB bandwidth:	26 MHz

Image rejection: 105 dB
432 MHz rejection: > 120 dB

The given data applies to the complete front-end. See also **fig. 9**.

Oscillator radiation from antenna input socket: − 94 dBm with module installed in receiver with covers on.

7.4. Intermodulation

Test-Equipment: 2 Sythesizer SMS, Power combiner ZSC 2 - 1 (MCL), Spectrum Analyser HP 141 T with 8553 B (HF) and 8552 B (IF), switched attenuator type 3023 (Weinschel).
Generator frequencies: 144.2 and 144.3 MHz, each − 10 dBm.
Mixer with DK 1 OF 046 / 047 but without pre-amp. 3rd order IP = 23 dBm.
Complete front-end:

switch pos. 1:	IP = − 2 dBm
switch pos. 2:	IP = + 1 dBm
switch pos. 3:	IP = + 2 dBm

The method of measurement is disdussed exhaustively in (5).

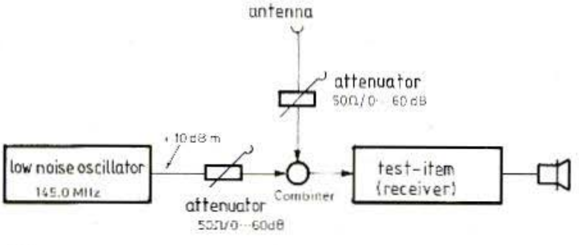

Fig. 10:
Suggested test set-up for blocking check

7.5. Blocking (Gain compression)

Mode: FM, BW: 15 kHz, test set-up as in **fig. 10**, switch pos. 1.

The signal noise of a wanted input signal is reduced from 10 dB to 0 dB when an interference signal, 100 kHz removed, reaches a power of − 11 dBm. The dynamic range can thus be calculated:

Noise floor of hyperthetical receiver of
NF = 0 dB and bandwidth 1 Hz = − 174 dBm

Noise floor of subject front-end with
NF = 1 dB and bandwidth 15 kHz = − 131 dBm

Signal input for 10 dB signal:
noise ratio = − 121 dBm

Interference signal input for 10 dB blocking (i. e. gain compression) = − 11 dBm

Dynamic range for 10 dB blocking
= (− 11 dB) − (− 121 dB) = 110 dB

7.6. Power requirements

A 15 VDC stabilised supply is required for this front-end, capable of delivering approx. 210 mA.

8. REFERENCES

(1) J. Kestler, DK 1 OF:
PLL Oscillators with Delay Lines, Part 3:
Oscillator Module for the 2-Metre Band
VHF COMMUNICATIONS Vol. 17, Ed. 2
Pages 112 - 120

(2) M. Martin, DJ 7 VY:
A New Type of Pre-Amplifier for 145 MHz and 435 MHz Receivers
VHF COMMUNICATIONS Vol. 10, Ed. 1
Pages 30 - 36

(3) M. Martin, DJ 7 VY:
A Modern Receive Converter for
2 m Receivers
VHF COMMUNICATIONS Vol. 10, Ed. 4
Pages 218 - 229

(4) J. Kestler, DK 1 OF:
Matching Circuits for Schottky
Ring Mixers
VHF COMMUNICATIONS Vol. 8, Ed. 1
Pages 13 - 18

(5) M. Martin, DJ 7 VY:
Empfängereingangsteil mit großem
Dynamikbereich
CQ DL 1975 Ed. 6, Pages 326 - 336

Jochen Jirmann, DB 1 NV and Friedrich Krug, DJ 3 RV

A Microcomputer-System for Radio Amateurs

Many readers will already be asking: "What's this then, a computer system specially for amateur use? Surely, commercial home-computers are so cheap that it's not worth the trouble building one".

Those, who have busied themselves with these things, will know that home computers have antiquated circuit concepts and have been pared down in order to make them as cheaply as possible. Also customer-specified integrated circuits are employed whose inner workings are, to some extent, a mystery. In order that the manufacturers' (expensive) peripheral equipment and cables are also sold, together with the computer, the connections are made as incomprehensible as possible. Difficulties always occur when home-made accessories and extensions are required to be added. Even if computer A is to be matched with printer B and disc drive C, the necessary cables and interface cards can, if one is unlucky, cost over half the price of the computer itself. Added to that comes the cost of additional books – a few hundred marks perhaps – in order that both the hardware and the software can be used advantageously together.Information which is actually more appropriate in the computer's handbook.

Standard interfaces, such as the Centronics printer interface, a serial V 24 connection, standardised drive system connections or a IEC–bus-interface could have made further extensions to the system much easier. A direct access to the processor bus is also desirable for experimental purposes. Unfortunately, it is not possible to find all the above mentioned connections on proprietry computer (the "Serial IEC–Bus" proclaimed by one manufacturer is more a "data brake" owing to an unbelievably slow information rate and is not suitable for serious use).

The data given about store capacity in home computers also must be taken with a pinch of salt because most of this is utilised immediately by the storage requirements of keyboard buffers, picture and graphic displays. A further sad chapter concerns the radio suppression measures which are dimensioned for the minimum consumer demands and the electronics packed into an unscreened plastic case making the use of any nearby sensitive receiver impossible.

These are all good reasons for considering the construction of a computer specially designed for the requirements of amateur radio.

One should keep his distance from component-saving concepts in which the CPU additionally samples the keyboard in multiplex operation and controls picture reproduction. Some of the single-board computers, propagated in a few magazines, are neither sure-fire of reproduce or capable of modification and adaption even if they have been successfully built. They are usually designed on a Euro-format printed circuit board and contain terminal and floppy controllers, the board being stacked with ICs, perhaps under a 40 legged IC a few 14 / 16 legged "beatles" will be hiding, or maybe the store elements are stacked in a tower and soldered to one-another.

It is much better that the computer has a compartmentalized system in which each module has a clearly defined role and transfer plane, and processed by a separate micro-processor. The operating system would use the universal Digital Research CP / M which allows an unproblematical software exchange between the hardware of various computers. The microcomputer-system developed by the university of Erlangen / Nürnberg is based on the Z 80 processor. The whole circuit has been planned so that it operates with CMOS circuits in order that, with suitable low-power consuming peripherals, battery operation is feasible.

The CMOS stores are, however, more than three times the price of the equivalent NMOS stores but posses the advantage of being uncritical in their use. Additionally, the store contents can be preserved with a small accumulator during times when the computer is shut-down.
The individual circuit elements are fitted onto simple Euro-cards with a reasonable packing density. An ECB-bus is employed as the system-bus which enables a multitude of non-system peripheral cards to be connected.

The computer consists of three basic units and a number of special-function cards. At the moment the following cards are in the testing process:

The CPU - card

This can also be employed independently as a control-computer for many purposes (e. g. antenna rotor- or radio relay / transponders control). It contains besides the Z 80-CPU two serial V 24-interfaces, a parallel 8-bit-interface from Centronics-Norm as well as a 16 kByte CMOS-RAM which is battery buffered. A 4 / 8 kByte EPROM contains a simple monitor program for the development of a simple machine program and for the charging of the CP / M from the floppy-disc station.

An alpha-numerical terminal card

This is normally connected to the serial terminal interface of the computer and can of course, be driven separately from the computer (serial data transmission).

This card contains a further Z 80 - CPU, a video controller MC 6845, a parallel keyboard input (Z 80 - PIO) and a serial computer interface. In this terminal it was the intention to forget everything which was not absolutely necessary (many manufactures put anything in, merely to utilise the EPROM capacity). Instead, we have put more effort into improving the picture quality.

The symbols are represented as a 7 x 12 matrix in a 9 x 14 field – a doubling of the picture elements of the usual 5 x 7 or 5 x 8 matrixes. Also, three display formats can be chosen by means of selector plugs; a 80 x 24 symbol format with an increased line-frequency (18 kHz) and two television standard formats with 64 x 16 symbols (for monitors) and 40 x 16 symbols (for TV with video input). As there is still enough space left over in the RAM and the EPROM there would be, in addition, a possible use of this card as an autonomous RTTY terminal. With the two cards already described, it is already possible to built a computer. If comprehensive mass storage and more RAM range (a further 40 K) is required, the following "store / floppy disc card" is required.

The store / floppy disc card

This contains a further 48 kByte CMOS memory which may be supported by a battery. CMOS memories are much dearer than dynamic NMOS-RAMs but the construction of the card is much easier owing to their simple control requirements (doesn't need address-multi-plexers and multiphase sync-generators). Also, the computer may be stopped at any time without losing information.

Dynamic stores, on the other hand must have the facility to be "re-activated" in order that all the capacitive store elements may preserve their information charges. Provisions must be made when using this type of store, to supply it from another source during shut-down if the store contents are required to be preserved. In amateur operations the processor may have to be switched off, for example, in order that the weakest radio signals are not drowned in computer hash.

The floppy-disc controller card uses the Western Digital WD 2793, a single-chip controller possessing a built-in analog PLL data separator. Its employment avoids the use of half the thirty or so chips usually used for this purpose and thereby utilising the card space more effectively.

All the popular 8 and 5 ¼ inch drives can be connected as well as compatible 3 ½ inch drives.
With the floppy-disc card the calculator is fully utilised as a CP / M computer with a 64 kByte RAM, a Centronics printer interface and a serial V 24 interface e. g. for computer to computer linking.

There are still a few additional cards in the test phase in which many users could find an interest:

a) A IEC-Bus card

This module contains the NEC 72 xx and enables the connection of test equipment, printers or other peripheral apparatus having an IEC / IEEE 488 / HP interface bus. Three sockets are provided on the PCB for 8 kByte EPROMs which can contain the IEC-bus control software.

b) A universal EPROM card

All the popular EPROMs up to 16 kBytes can be programmed with this card and two zero-force sockets are provided for a readable and programmable EPROM.

c) A ROM software card

If the re-loading of extensive programs from the diskette is to be avoided and if the floppy-disc is not convenient, the ROM in the software card can accomodate 64 kByte in eight 8 kByte EPROMs. This card uses the top 8 K of the store leaving only 56 kBytes RAM for the user's disposal. By means of a control circuit, the top 8 K can be gated by any selected 8 kByte EPROM which can be read-off. Many readers will be asking themselves: "Where is the terminal card devoted to the representation of graphics?" A Thomson-CSF graphic processor, the EF 9366 / 67 is available, but its alphanumerical presentation would satisfy only modest demands. The authors have therefore decided that a purely graphic card with a further processor and a 64 kByte dynamic picture store should be developed to work in parallel with the alpha-numeric card. The resolution amounts to 720 x 320 pixels and the graphic video signal is mapped with the normal alphanumeric video. The necessary synchronisation and strobing signals will be taken from the alpha card.

Power supplies

In order to make the computer work, a suitable power supply is necessary. A power supply has been developed which is capable of supplying the computer together with two 5 ¼ inch drives and a monochrome monitor. It delivers 5 V / 7 A, 12 V / 3 A (6 A peak) and – 12 V / 0. 1 A for the V 24 interface.

Particular attention was paid to the rfi suppression in order that hash does not find its way into a neighbouring receiver neither by direct radiation nor by being fed from the computer via the mains. The radio transmitter should not be allowed to throw the computer into disarray. A further speciality is that all signals in the computer are derived from a 16 MHz synchronizing generator. It is then possible to frequency-lock this with a radio time signal DCF 77 etc. which is a necessary condition for a coherent transmission mode. The modules DJ3RV 006 ..... 007 can be regarded as being the first peripherals of the amateur computer introduced by this article.

It is intended to give a short description of the computer sub-units in the following editions of VHF-COMMUNICATIONS.

MATERIAL PRICE LIST OF EQUIPMENT

described in edition 4 / 85 of VHF COMMUNICATIONS

DK 1 OF	**Two-Metre Receiver Front-End**		Art.Nr.	**Ed. 4 / 1985**
PC-board	DK 1 OF 048	double-sided, thro' plated	6935	DM 29.—
PC-board	DK 1 OF 049	double-sided, thro' plated	6936	DM 36.—
Components	DK 1 OF 048 / 049	4 FETs, 1 FET-Op Amp 2 PIN diodes, 2 Ge-diodes, 1 ringmixer SRA - 1 H or TAK - 1 WH, 5 ceramic and 7 foil trimmers, 1 tantalum, 13 F / T caps. 9 ceramic discs and 25 ceramic de-coup. caps., silvered wire, 1 ferrite bead, 7 chokes, 1 pre-set and 32 resistors	6937	DM 268.—
Kit	**DK 1 OF 048 / 049**	**complete with all above parts**	**6938**	**DM 325.—**
DJ 1 EE	**SSB Mini-Transverter 144 / 1296 MHz**			**Ed. 4 / 1985**
PC-board	DJ 1 EE 005	double-sided, not bored, silvered, without comp. plan	6939	DM 25.—
PC-board	DJ 1 EE 005	10 transistors, 8 diodes, 2 PIN diodes, 4 H / C diodes, 1 microwave trimmer, 13 foil trimmers, 6 chip and 25 disc F / T caps., 1 tant. and 1 elect., 4 F / T and 29 ceramic capacitors, 1 pre-set and 34 resistors, 1 twin-hole bead, 3 sorts of wire, 10 mini chokes, 1 m teflon coax. cable, 1 relay, 1 tin-plate box, 2 BNC single-hole sockets	6940	DM 459.—
Crystal	96,000 MHz HC - 43 / U		6224	DM 26.—
Kit	**DJ 1 EE 005**	**complete with all above parts**	**6941**	**DM 490.—**
DB 1 NV	**12 V-Mobile Switched-Mode-Power-Supply**			**Ed. 2+3/85**
PC-board	DB 1 NV 002	single-sided, drilled, with comp. plan	6932	DM 83.—

Under Development: Interface slave 10

Fully-automatic antenna tracking system for satellite communication

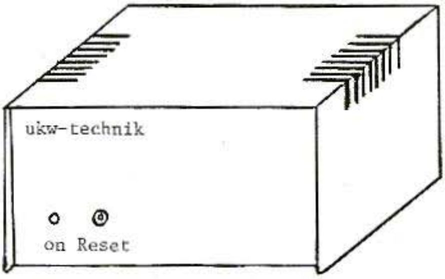

for the satellite-rotor-systems
KR 5400
KR 5600

Stock-No. 1001 DM 590.—

This interface, together with a personal computer and KR 5000 series control system, enables the exact positioning of the antenna to be carried out. The positioning pre-set data is provided in ASCII-code from the serial interface.

During both horizontal and vertical rotations, the actual antenna position can be interrogated as often as desired. Apart from the commands "pre-set position" and "interrogate position" the interface processes a series of further commands such as, left, right, stop.

The resolution of the twin-channel A / D converter amounts to 10 bit. This, converted, results in a setting accuracy of 0.35° horizontal and 0.18° vertical. Existing control-boxes can be suitably modified.

Which Volumes of VHF COMMUNICATIONS are missing from your library?

As you know, the publishers continue to reprint back copies of VHF COMMUNICATIONS. Since they are full technical articles and little news or advertising, they contain a great deal of non-again information that is just as valid today. Many of our readers will also have lent out copies of VHF COMMUNICATIONS and never received them back. All editions available can be obtained from your representative or from the publishers.

Subscription to VHF COMMUNICATIONS 1985/1986	**each DM 24.00**
VHF COMMUNICATIONS – Volume 1983/1984	each DM 22.00
VHF COMMUNICATIONS – Volume 1981/1982	each DM 20.00
VHF COMMUNICATIONS – Volume 1979/1980	each DM 18.00
VHF COMMUNICATIONS – Volume 1976, 1977, and 1978	each DM 16.00
VHF COMMUNICATIONS – Volume 1975	DM 14.00
VHF COMMUNICATIONS - Individual copies 1985/1986	each DM 7.00
VHF COMMUNICATIONS - Individual copies 1983/1984	each DM 6.50
VHF COMMUNICATIONS - Individual copies 1981/1982	each DM 5.50
VHF COMMUNICATIONS – Individual copies 1979/1980	each DM 4.50
VHF COMMUNICATIONS – Individual copies 1975,1976,1977,1978	DM 4.00

Individual copies out of elder, incomplete volumes, as long as stock lasts:

1/1970, 2/1970, 2/1971, 1/1972, 2/1972, 4/1972	each DM 3.00
2/1973, 4/1973, 1/1974, 2/1974, 3/1974	each DM 3.00

VHF COMMUNICATIONS – Discount price for any 3 volumes including 1 binder:

VHF COMMUNICATIONS – Volumes 1975 – 1977	DM 47.00
VHF COMMUNICATIONS – Volumes 1976 – 1978	DM 48.00
VHF COMMUNICATIONS – Volumes 1977 – 1979	DM 50.00
VHF COMMUNICATIONS – Volumes 1978 – 1980	DM 52.00
VHF COMMUNICATIONS – Volumes 1979 – 1981	DM 56.00
VHF COMMUNICATIONS – Volumes 1980 – 1982	DM 59.00
VHF COMMUNICATIONS – Volumes 1981 – 1983	DM 62.00
VHF COMMUNICATIONS – Volumes 1982 – 1984	DM 68.00
VHF COMMUNICATIONS – Volumes 1983 – 1985	DM 72.00
Plastic binder for 3 volumes	DM 8.00

All prices including surface mail.

UKW**berichte** Terry D. Bittan · Jahnstr. 14 · Postfach 80 · D-8523 Baiersdorf
Tel. West Germany 9133-855. For Representatives see cover page 2

Space and Astronomical Slides

Informative and Impressive

VHF COMMUNICATIONS now offers sets of phantastic slides made during the Gemini, Apollo, Mariner, and Voyager missions, as well as slides from leading observatories. These are standard size 5 cm x 5 cm slides which are framed and annotated.
Prices plus DM 3.00 for post and packing.

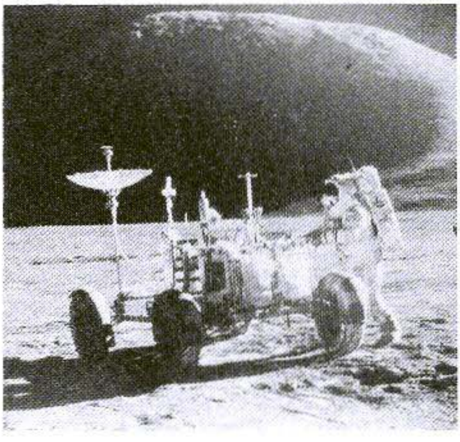

Sets of 5 NASA-slides DM 8.50 per set

Set 8103	Apollo 11: Earth and Moon
Set 8104	Apollo 11: Man of the Moon
Set 8105	Apollo 9 and 10: Moon Rehearsal
Set 8106	From California to Cap Canaveral
Set 8107	Apollo 12: Moon Revisited
Set 8108	Gemini Earth Views
Set 8109	Apollo 15: Roving Hadley Rille
Set 8110	Apollo 16: Into the Highlands
Set 8111	Apollo 17: Last voyage to the moon
Set 8112	Apollo 17: Last Moon Walks
Set 8113	Mariner 10: Mercury and Venus

Set 8147 »Jupiter encountered« 20 slides of VOYAGER 1 & 2 DM 35.00

1. Jupiter and 3 satellites 2. The giant planet 3. Jupiter, Io and Europa 4. The Red spot 5. The Red spot in detail 6. The swirling clouds 7. Io and a white oval 8. The neighbourhood of the Red spot 9. The rings of Jupiter 10. The Gallilean satellites 11. Amalthea 12. Callisto 13. Impact feature on Callisto 14. Eruption on Io 15. Io full disc 16. Europa close-up 17. Europa distant view 18. Ganymede close-up 19. A distant Ganymede 20. The Iovian system

Set 8100 »Saturn encountered«, 20 VOYAGER-1 slides DM 35.00

1. Saturn and 6 of its moons 2. Saturn from 11 mio miles 3. Saturn from 8 mio miles 4. Saturn from 1 mio miles 5. Saturn and rings from 900.000 miles 6. Saturn's Red spot 7. Cloud belts in detail 8. Dions against Saturn 9. Dione close-up 10. Rhea 11. Craters of Rhea 12. Titan 13. Titan's polar hood 14. Huge crater on Mimas 15. Other side of Mimas 16. Approaching the rings 17. Under the rings 18. Below the rings 19. »Braided« F ring 20. Iapetus

Set 8148 »VOYAGER 2 at Saturn«, 20 VOYAGER-2 slides DM 35.00

1. VOYAGER 2 approaches 2. Clouds & rings 3. Storms & satellites 4. Cyclones, spots & jet streams 5. Convective regions 6. Atmospheric disturbance 7. Rings & shadows 8. The »C« ring 9. Ring details 10. The »A« ring 11. Looking back on Saturn 12. Titan – night side 13. Titan – atmospheric bands 14. The »F« ring 15. Hyperion close-up 16. Iapetus revealed 17. Enceladus explored 18. The Tethys canyon 19. The »F« ring structure 20. Within the Enke division

Set 8102 »The Solar System«, 20 NASA/JPL slides DM 35.00

1. Solar System 2. Formation of the Planets 3. The Sun 4. Mercury 5. Crescent Venus 6. Clouds of Venus 7. Earth 8. Full Moon 9. Mars 10. Mars: Olympus Mons 11. Mars: Grand Canyon 12. Mars: Sinuous Channel 13. Phobos 14. Jupiter with Moons 15. Jupiter Red Spot 16. Saturn 17. Saturn Rings 18. Uranus and Neptune 19. Pluto 20. Comet Ikeya-Seki.

Set 8149 »The Sun in action«, 20 NASA/JPL slides DM 35.00

1. Sun in Hα light 2. Total Solar eclipse 3. Outer corona 4. Corona from SMM satellite 5. Corona close-up 6. Solar magnetogram 7. Active regions in X-radiation 8. X-ray corona 9. A coronal hole 10. Solar flare 11. Active Sun 12. Eruptive prominence 13. Gargantuan prominence 14. Eruptive prominence 15. Huge Solar explosion 16. Prominence in action 17. Sun in action 18. Magnetic field loops 19. Prominence close-up 20. Chromospheric spray

Set 8144 »Space shuttle«, 12 first-flight slides DM 24.00

1. STS1 heads aloft 2. View from the tower 3. Tower clear 4. Launch profile 5. Payload bay open 6. STS control Houston 7. In orbit, earth seen through the windows 8. Bob Crippen in mid-deck 9. John Young 10. Approaching touchdown 11. After 54.5 hours in space Columbia returns to Earth. 12. Astronauts Crippen and Young emerge after the successful mission

Set 8150 »Stars and Galaxies«, 30 astro color slides, AAT 1977 – 1982, DM 46.00

1. The Anglo-Australian 3.9 m Telescope (AAT) 2. AAT Dome 3. Telescope Control Console 4. An Observer at the Prime Focus 5. Star Trails in the SW 6. Circumpolar Star Trails 7. Centaurus A, NGC5128 8. The Spiral Galaxy M83 (NGC5236) 9. The Eta Carinae Nebula 10. An open Cluster of Stars NGC3293 11. A Planetary Nebula, NGC6302 12. The Trifid Nebula M20 (NGC6514) 13. The Cone Nebula 14. S Monocerotis and NGC2264 15. The Helix Nebula, NGC7293 16. A Wolf-Rayet Star in NGC2359 17. A Spiral Galaxy NGC2997 18. Messier 16 (NGC6611) 19. The Orion Nebula 20. Dust and Gas in Sagittarius, NGC6589-90 21. NGC6164/5. The Nebulosity Around HD148937 22. Dust Cloud and Open Cluster NGC6520 23. The Spiral Galaxy NGC253 24. A Mass-Loss Star, IC2220 25. The Jewel Box NGC4755 26. Local Group Galaxy NGC6822 27. Central Regions of NGC5128 28. Towards the Galactic Centre 29. The Trapezium 30. The Trifid Stars

UKW berichte Terry D. Bittan · Jahnstr. 14 · Postfach 80 · D-8523 Baiersdorf
Tel. West Germany 9133-855. For Representatives see cover page 2